Response to Referees

We thank the reviewers for their careful reading and their constructive comments on our manuscript. As detailed below, the reviewer's comments are shown as italicized font, our response to the comments are normal font. New or modified text is in blue.

Referee #1

This paper presents NO_3 and N_2O_5 observational data from a suburban site in Beijing during the summer of 2016. The authors use these data to investigate the oxidation of volatile organic compounds (VOC) by NO_3 and the effect of N_2O_5 heterogeneous uptake on reactive nitrogen loss and $ClNO_2$ production in the Beijing urban outflow. Nocturnal biogenic VOC oxidation was shown to be dominated by NO_3, and the heterogeneous uptake of N_2O_5 was found to be a significant loss mechanism for reactive nitrogen. The uptake of N_2O_5 was found to produce approximately a factor of four more inorganic nitrate than organic nitrate from the NO_3 + VOC pathway and result in significant $ClNO_2$ production. These results are compared, and broadly agree, with previously reported observations and represent a valuable contribution to the growing body of work on the importance of nocturnal chemistry on local atmospheric composition. I recommend publication of the manuscript once the following minor comments /technical corrections have been addressed.

Thanks for the referee's positive and helpful comments.

Minor comments / technical corrections.

1. Lines 60-61: Please could the author state if these are mass or molar yields.

These are the mass yields, and we added the explanation in the text.

Changed in line 60-61: "The reaction of NO_3 with isoprene has a SOA mass yield of 23.8% (Ng et al., 2008). For the reaction with monoterpene, such as limonene, the SOA mass yield can reach 174% at ambient temperatures (Boyd et al., 2017)."

2. Line 148-150 – It would be easier for the reader if the authors could be consistent with the order of N_2O_5 and $ClNO_2$ in this sentence.

Thanks for the suggestion, we now changed units of both N_2O_5 and $ClNO_2$ to "pptv".

3. Figure 3: The scale on the NO plot makes it difficult to see NO mixing ratios. Please consider either a log scale or a discontinuity to make this more visible.

We changed to log scale accordingly, and we labelled 0.06 ppbv NO in the black line in Figure 2 in the revised manuscript.

4. Lines 276-278: This sentence is confusing, please restructure.

We rewrote as: "The N_2O_5 concentration was highly correlated with NO_2 (R^2 = 0.81) and the NO_3 production rate (R^2 = 0.60), suggests the N_2O_5 concentration was solely response to the NO_2 concentration in the background air mass when enough O_3 is presented."

5. Line 289: Please re-reference the recent studies in the NCP.

We re-cited the recent studies in the NCP in Line 289 as suggested: "Tham et al., 2016; X. F. Wang et al., 2017; Z. Wang et al., 2017".

6. Figure 8 and lines 389 – 392: There is an inconsistency between the text and Fig. 8. In the text the authors state that on the three days with the largest discrepancies between the steady state calculated N_2O_5 lifetime and that calculated using the overall k(N_2O_5) the steady state calculation is much higher than the overall k(N_2O_5). In Fig. 8 however, the discrepancy on 30th May is in the opposite direction, with the steady state lifetime approaching a factor of 2 lower than the overall k(N_2O_5). The authors should correct this statement and provide an explanation for this discrepancy. The authors should also explain why there is no steady state calculated N_2O_5 lifetime for 31st May in Fig. 8.

For the night of 29th-30th May (Referee quoted as 30th May), the calculated steady state loss rate constant of N_2O_5 is much smaller than that of the overall k(N_2O_5). We agree with the reviewer that this discrepancy needs more explanations. Considering that the large uncertainties propagated from the observed parameters (e.g., NO_2, N_2O_5, S_a), the discrepancies between the calculated steady state loss rate constant of N_2O_5 and the overall k(N_2O_5) is mostly within the estimated uncertainty levels. The steady state loss rate constant on the night of 30th May (mentioned 31th May in the comment) was calculated in fact, but the values are much higher than 0.02, the reason of high steady state loss rate constant on the night of 30th - 31th May was not well

understand. In the revised manuscript, we enlarged the y-axis and changed to log scale, as well as added the error bar of the estimated uncertainties in the Figure 7.

Change in the revised manuscript:

"Figure 7 shows the time series of the overall N_2O_5 loss rate constant as well as the N_2O_5 steady state loss rate constant. The overall N_2O_5 loss rate constant was calculated from the individual terms (Eq.3). The uncertainties of the N_2O_5 steady state loss rate constant and the overall $k(N_2O_5)$ are estimated to be 67% and 95%, respectively (Eq. 7 and Eq. 8). The largest error sources were from the corrected NO_2 measurements so that it is really important to have accurate NO_2 measurement instrument involved in the future campaigns.

$$\frac{\Delta Lss(N_2O_5)}{Lss(N_2O_5)} = \sqrt{(\frac{\Delta[N_2O_5]}{[N_2O_5]})^2 + (\frac{\Delta[NO_2]}{[NO_2]})^2 + (\frac{\Delta[O_3]}{[O_3]})^2 + (\frac{\Delta K_{eq}}{K_{eq}})^2} \quad \text{(Eq. 7)}$$

$$\frac{\Delta k(N_2O_5)}{k(N_2O_5)} = \sqrt{(\frac{\Delta[N_2O_5]}{[N_2O_5]})^2 + (\frac{\Delta[S_a]}{[S_a]})^2 + (\frac{\Delta[\gamma]}{[\gamma]})^2 + (\frac{\Delta[NO_2]}{[NO_2]})^2 + (\frac{\Delta[O_3]}{[O_3]})^2 + (\frac{\Delta[VOC_s]}{[VOC_s]})^2 + (\frac{\Delta K_{eq}}{K_{eq}})^2} \quad \text{(Eq. 8)}$$

On the night of 29 May, the steady state loss rate constant was much lower than the overall $k(N_2O_5)$; on the nights of 28, May and 3 June, the $L_{ss}(N_2O_5)$ calculated by the steady state method were much higher than the overall $k(N_2O_5)$, but these discrepancies were in the range of the uncertainties. Except the case happened on the night of 30 May, when the steady state loss rate constant was about ten times higher than the overall loss rate constant, and the reason was not well understood according to the available parameters that we have detected. In general, the overall N_2O_5 loss rate constant and the steady state N_2O_5 loss rate constant were comparable taking into considerations of the uncertainties. "

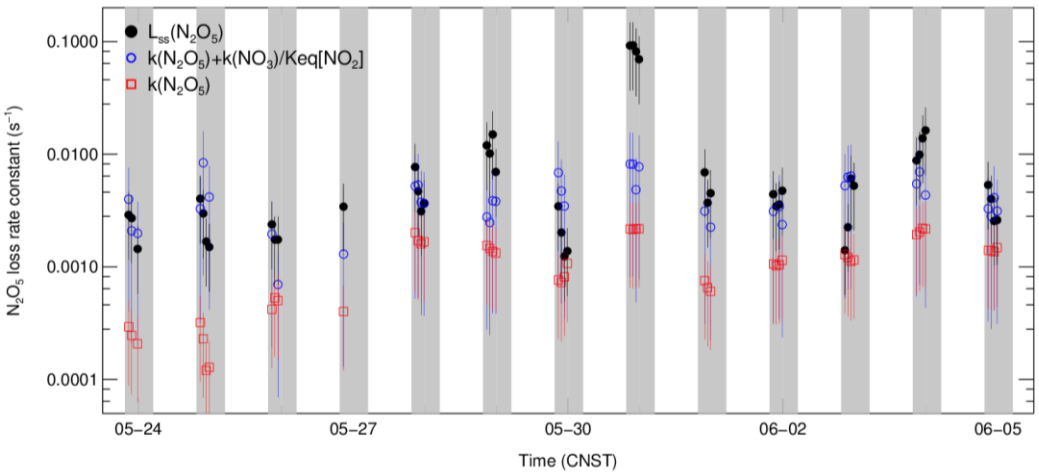

Figure 7. Time series of the individual N_2O_5 loss terms and the loss rate constant of N_2O_5 in steady state ($L_{ss}(N_2O_5)$).

7. Figure 9: Although the acronyms used in the x-axis labels are described in the text, it would help the reader if they were re-stated in the figure caption.

Added the description in the caption of Figure. 9 as following: "The nighttime VOCs reactivity of NO_3 and O_3 (defined as the pseudo first order loss rate of VOCs initialed by oxidants, include NO_3 and O_3); the VOCs are classified as isoprene (ISO), monoterpene **(**MNT), the terminal alkenes (OLT) and the internal alkenes (OLI)**.** The data were selected from 20:00 to the next day 04:00."

8. Line 301 and Table 3: Please check that X. F. Wang and Z. Wang references are correct.

We corrected the reference accordingly. The study conducted in Mt. Tai, China was from Z. Wang et al., 2017 and the study conducted in Jinan, China was from Z. Wang et al., 2017

Referee #2

Wang et al present measurements of N_2O_5, $ClNO_2$ and ancillary species in the urban outflow of Beijing and thereby analyze nocturnal rates of oxidation of VOCS, NOx lifetimes and chlorine activation via heterogeneous reaction of N_2O_5 on chloride containing particles. N_2O_5 uptake coefficients were in the "usual" range and $ClNO_2$ yields were high, implying abundant sources of chlorine. The authors use established expressions to analyze their data and the manuscript contributes to the growing literature on nighttime VOC oxidation, NO_x loss and $ClNO_2$ formation without providing significant new insight. Detracting from this work, much of the referencing seems to be an arbitrary selection (often self-citation) of related work and the estimation (or presentation) of uncertainties in derived parameters is largely missing. The following points should be addressed (some are major) and the English language corrected (some suggestions are listed below) before re-review.

Thanks for the referee's careful and constructive comments. We checked and cited the references carefully in the revised manuscript. The uncertainties analysis was added as suggested.

1. L61 State how the yield of SOA (23.8 % or 174 %) is defined.

These are the mass yields, and we revised accordingly in the text. Change in the revised text: "The reaction of NO_3 with isoprene has a SOA mass yield of 23.8% (Ng et al., 2008). For the reaction with a monoterpene, such as limonene, the SOA mass yield can reach 174% at ambient temperatures (Boyd et al., 2017)."

2. L70 kN_2O_5 is not a rate coefficient. Its best to call it a pseudo-first order loss rate constant to avoid confusing it with rate constants for gas-phase reactions.

We change accordingly.

3. L70 Eq. (1) was certainly not derived by Tang et al in 2017. Use an appropriate (earlier) reference.

We cited the reference: "Wahner et al., 1998".

4. L175 The correction factor of 0.6 (independent of time of day, day of campaign, NO_x, or air mass-age) is clearly a poor assumption given that the NO_x to NO_y ratio is highly variable in time and space. The assumption that the correction factor in Wangdu is the same as in Changping is without real basis. Note also that the photo-stationary state between NO, NO_2 and O_3 will break down in the presence of other oxidants (e.g. RO_2) so that measurement of NO and O_3 (and j-NO_2) cannot replace NO_2 measurements. The authors must estimate the uncertainty related to this correction factor (and thus with the NO_2 measurements) is they wish to use NO_2 data in any quantitative sense. This applies to section 4.2 where they calculate N_2O_5 lifetimes in steady state via calculation of the N_2O_5 production term, which requires NO_2 mixing ratios. It also applies to the calculation of NO_3 from the N_2O_5 and NO_2 measurements and the equilibrium constant and this impacts on the results of section 4.2 where NO_3 concentrations are used to calculated oxidation rates of VOCs. In principal, the lack of accurate NO_2 measurements during this campaign reduces many conclusions of this paper to a qualitative level.

According to the reviewer's suggestions, we now extensively evaluated the influence of the uncertainty of the used NO_2 concentrations on the deduced VOCs (+NO_3) and N_2O_5 reactivity.

Line 177: "The correction factor (0.6) used to be the averaged scaled value of the correction factors during nighttime, the standard deviation of the daytime correction factor for all the air masses experienced at Changping site was determined to be 0.27 (1σ), which extended to nighttime and result in an uncertainty of correction to be 45%. The uncertainty of NO_2 is therefore about 50% when further included the associated measurement uncertainty from calibrations."

According to a Gaussian error propagation approach (see the following equations), the uncertainties of the calculated steady state lifetime, the overall k(N_2O_5) and the NO_3 concentration were determined to be 67%, 95% and 67%, respectively.

We revised the paper correspondingly as follows:

Firstly, changed in line 242: "the uncertainty of NO_3 calculation was estimated to be 67% according to Eq. 2 which is dominated by uncertainty of the NO_2 concentrations.

$$\frac{\Delta[NO_3]}{[NO_3]} = \sqrt{\left(\frac{\Delta[N_2O_5]}{[N_2O_5]}\right)^2 + \left(\frac{\Delta[NO_2]}{[NO_2]}\right)^2 + \left(\frac{\Delta[O_3]}{[O_3]}\right)^2 + \left(\frac{\Delta K_{eq}}{K_{eq}}\right)^2} \quad \text{(Eq. 2)"}$$

Secondly, the N_2O_5 loss rate constant was revised in Figure 7, the error bar was added to denote the uncertainties of N_2O_5 steady state loss constant and the overall N_2O_5 loss rate constant (as NO_2 concentration affected the contribution of NO_3 oxidation).

Changed in line 390: "Figure 7 shows the time series of the overall N_2O_5 loss rate constant as well as the N_2O_5 steady state loss rate constant. The overall N_2O_5 loss rate constant was calculated from the individual terms (Eq.3). The uncertainties of the N_2O_5 steady state loss rate constant and the overall k(N_2O_5) are estimated to be 67% and 95%, respectively (Eq. 7 and Eq. 8). The largest error sources were from the corrected NO_2 measurements so that it is really important to have accurate NO_2 measurement instrument involved in the future campaigns.

$$\frac{\Delta Lss(N_2O_5)}{Lss(N_2O_5)} = \sqrt{\left(\frac{\Delta[N_2O_5]}{[N_2O_5]}\right)^2 + \left(\frac{\Delta[NO_2]}{[NO_2]}\right)^2 + \left(\frac{\Delta[O_3]}{[O_3]}\right)^2 + \left(\frac{\Delta K_{eq}}{K_{eq}}\right)^2} \quad \text{(Eq. 7)}$$

$$\frac{\Delta k(N_2O_5)}{k(N_2O_5)} = \sqrt{\left(\frac{\Delta[N_2O_5]}{[N_2O_5]}\right)^2 + \left(\frac{\Delta[S_a]}{[S_a]}\right)^2 + \left(\frac{\Delta[\gamma]}{[\gamma]}\right)^2 + \left(\frac{\Delta[NO_2]}{[NO_2]}\right)^2 + \left(\frac{\Delta[O_3]}{[O_3]}\right)^2 + \left(\frac{\Delta[VOC_s]}{[VOC_s]}\right)^2 + \left(\frac{\Delta K_{eq}}{K_{eq}}\right)^2} \quad \text{(Eq. 8)}$$

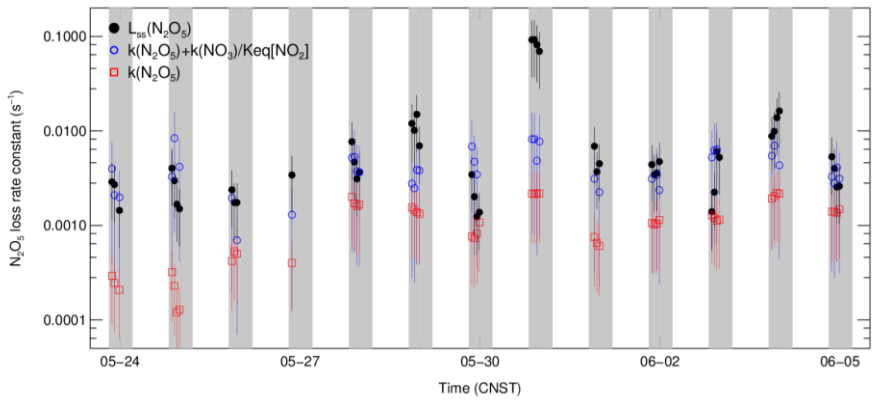

Figure 7. Time series of the individual N_2O_5 loss terms and the loss rate constant of N_2O_5 in steady state ($Lss(N_2O_5)$).

Thirdly, the uncertainty of VOCs loss rate by NO_3 was added in the Figure 8. Changed in line 422: "Previous measurement indicated the main detectable monoterpenes were α-pinene and β-pinene in summer Beijing (personal communication with Ying Liu). Here we assumed α-pinene and β-pinene contributes equally to the mixing ratios of the monoterpenes. The average value of the rate coefficients of α-pinene and β-pinene with NO_3 (Atkinson and Arey, 2003) was used as the rate coefficient of monoterpene with NO_3. The uncertainty of the monoterpene + NO_3 rate coefficient in these air masses is thus estimated to be 50%. Since the uncertainty of calculated NO_3 is estimated to be 67%, the overall uncertainty of monoterpene reactivity toward NO_3 was calculated to be 85% according to a Gaussian propagation method, the uncertainties of other VOCs reactivity toward NO_3 was calculated to be 75% by assuming the uncertainties of the corresponding bimolecular rate constants to be 30%."

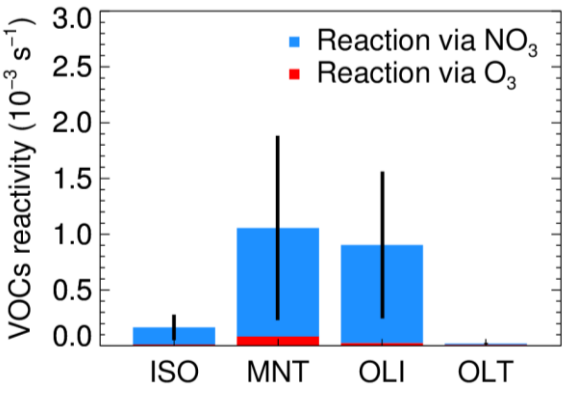

Figure 8. The nighttime VOCs reactivity of NO_3 and O_3 (defined as the pseudo first order loss rate of VOCs initialed by oxidants, include NO_3 and O_3); the VOCs classified as isoprene (ISO), monoterpene (MNT), the terminal alkenes (OLT) and the internal alkenes (OLI). The data were selected from 20:00 to the next day 04:00.

5. L191 "Figure 2 shows the calculated backward trajectories using the Hybrid Single Particle Lagrangian Integrated Trajectory (HYSPLIT) model". As far as I can tell, this is the first and last mention of air-mass trajectories. I would suggest that the Figure can be relegated to the SI.

We changed accordingly.

6. L235 "The single peak (in N_2O_5) occurred near 20:00 and then gradually decreased". Is this a reproducible feature of the campaign or a bias of the mean due to one or two events. Taking the median rather than the mean would resolve this. Also, why (line 236) does the N_2O_5 increase before sunrise (or do the authors mean "at sunrise")?

Thanks for the suggestion, we checked the median value of N_2O_5 and NO_3, the peak also occurred near 20:00. Therefore, we rewrote the description as following: "A peak occurred near 20:00 and decreased below the instrument detection limit at sunrise". We corrected to "at sunrise" in Line 236 accordingly.

7. L243-246 "$ClNO_2$ accumulated corresponding to N_2O_5 after sunset but $ClNO_2$ peaked in the middle or the second half of the night since the nocturnal sinks of $ClNO_2$ were negligible to our knowledge." I'm not sure what the authors are trying to say here.

We rewrote the sentence as following: "The observed $ClNO_2$ concentrations showed a clear increase after sunset and reached a maximum before sunrise for BAM period while reached a maximum around midnight for the UAM period."

There are many examples that show great variability in the N_2O_5–to-$ClNO_2$ ratio. The interesting part of this section (lines 243 to 267) is the discussion of the sources of chloride needed to drive the $ClNO_2$ formation in this continental region. In principal, the chloride content of the aerosol can be calculated from the yield of $ClNO_2$ and the appropriate expression that defines the parameter "f". I suggest the authors do this.

Thanks for the suggestion. We added the following discussion in the revised text: "The required nocturnal source of Cl^- to support the $ClNO_2$ production is further estimated through its loss rate. The $\gamma \times f$ was set to the campaign average value (0.019) (see Sect. 4.1), and real-time Cl^- loss rate via N_2O_5 can be calculated based on the measured N_2O_5 and Sa by Eq.3.

$$L[Cl^-] = (\gamma \times f) \cdot \int_{t_{sunset}}^{t_{sunrise}} \frac{C \cdot S_a}{4} [N_2O_5] dt \qquad \text{(Eq. 3)}$$

Here the $L(Cl^-)$ denotes the integral Cl^- loss to form the $ClNO_2$ per night. The required source term of the Cl^- need to support the $ClNO_2$ formation during the campaign was range from (0.5 - 4.0 ppbv per night) with (1.7 ± 2.3 ppbv per night) on average. The gas phase HCl predicted by the ISORROPIA II model showed that the HCl concentration near sunset period was high enough (much larger than 2 ppbv) to support the $ClNO_2$ formation (Figure. S3).

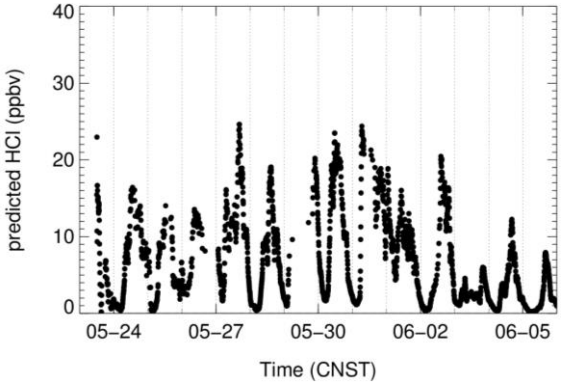

Figure S3. The predicted gas phase HCl concentrations by ISORRPIA II model."

L249 and promoted the N_2O_5 conversion to $ClNO_2$ (e.g., Roberts et al., 2009). Why this citation? The formation of $ClNO_2$ from N_2O_5 was known (and quantified) long before 2009. Cite the appropriate literature.

Corrected the citation as following: "Finlayson-Pitts et al., 1989; Behnke et al., 1997"

8. L279 In lines 280-290. It is not clear whether we are dealing with ratios of the concentrations of $ClNO_2$ and N_2O_5 or ratios in their production rates (L282). If relative rates are calculated we need to know over which period they were derived.

The daily average or median ratio of the mixing ratio of $ClNO_2$ to N_2O_5 was calculated from 20:00 to the next day 04:00, and the ratio of their production rates was not calculated here.

Revised the description as following: "We used the concentration ratio of $ClNO_2$ to N_2O_5, to describe the conversion capacity of N_2O_5 to $ClNO_2$. The nighttime peak values and mean values of $ClNO_2$: N_2O_5 were used to calculate the ratios are listed in Table S2, the calculation period is from 19:30 to the next day 05:00."

9. L295 A composite term, $\gamma \times f$, was used to evaluate the overall $ClNO_2$ yield (f). . . . .

The sentence was rewrote as following: "A composite term, $\gamma \times f$, was used to evaluate the production of $ClNO_2$ from N_2O_5 heterogeneous hydrolysis (Mielke et al., 2013)"

10. L296 How and over what period was the production rate of $ClNO_2$ determined? How stable were N_2O_5 and S_a in this period? L296 the term was estimated by considering. Give the expression used to derive the composite term from the observables.

In the revised paper, we added the expression and the corresponding explanation to derive the composite term, $\gamma \times f$, as the following:

"The term, $\gamma \times f$, was estimated by fitting the observed $ClNO_2$ in a time period when the nighttime concentrations of $ClNO_2$ kept increasing. The increased $ClNO_2$ was assumed to be solely from the N_2O_5 uptake. The fitting was optimized by changing the input of $\gamma \times f$ associated with the measured N_2O_5 and S_a, until the $ClNO_2$ increasing was well reproduced (Eq. 4). Here t_0 and t denote the start time and end time, respectively, $[ClNO_2](t_0)$ is the observed concentration at t_0 and set as the fitting offset. The calculation time duration was normally several hours, and the derived $\gamma \times f$ was found to be constant with small uncertainties for optimization (see Table S3) (e.g., a case showed in the following Figure A1). It is worth to be noticed that both the N_2O_5 and S_a is not necessary to be stable in this calculation due to the use of integration.

$$[ClNO_2](t) = [ClNO_2](t_0) + (\gamma \times f) \cdot \int_{t_0}^{t} \frac{c \cdot S_a}{4} [N_2O_5]\,dt \qquad \text{(Eq. 4)}$$

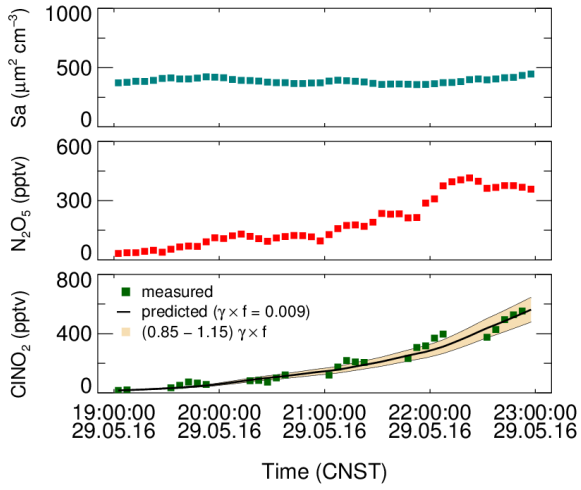

Figure A1. The reproduction of $ClNO_2$ by observed N_2O_5 and S_a.

11. L300 and 301 (and Table 3) the average values need to be listed with standard deviations to enable comparison. The same applies to Table 4.

The standard deviation of this study was added in both Table 3 and Table 4.

12. L313 uptake coefficients are derived from analysis of particulate nitrate and $ClNO_2$ concentrations. Only those nights were chosen when a clear covariance between these parameters was observed. The authors should explain how they define "clear covariance" and why, on other nights, covariance did not exist.

Here the "clear covariance" is pointing to the conditions when the square of the correlation coefficient is larger than 0.5 ($R^2 > 0.5$). Changed in line 313: "For some nights, significant correlations between pNO_3^- and $ClNO_2$ were presented ($R^2 > 0.5$); while on the other nights, the R^2 were always smaller than 0.2, which is not meet the theoretical hypothesis of this method. In this case, we chose the nights with high correlations."

The reasons for the significant different correlations presented between the two groups of nights are still unclear. We did not find any observed parameters to explain the difference.

Surely the formation of $ClNO_2$ must always be accompanied by formation of particle nitrate? A major issue in this analysis is the assumption that the particulate nitrate is only formed from N_2O_5 uptake and not influenced by (temperature dependent) HNO_3 repartitioning. It appears that there were no measurements of gas-phase HNO_3 or ammonia to support the contentions that this was not important. The authors must assess this rigorously and state how the uptake coefficients would be influenced by HNO_3 uptake.

Unfortunately, we did not have the gas-phase HNO_3 or ammonia during this campaign. Our deduction on this point is as the follows,

Firstly, the daytime produced HNO_3 will soon be in equilibrium with the particulate nitrate within a time scale of about hundred seconds so that the daytime influence will be removed at the very beginning at night (cf. Figure A2, the observations of HNO_3 at summer Beijing in 2015).

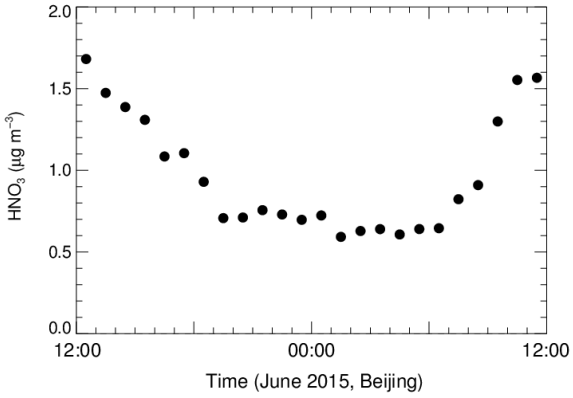

Figure A2. The mean diurnal variation of HNO_3 during a campaign conducted in June 2016 in urban Beijing.

Secondly, we think the nighttime production of HNO_3 is very small mainly due to the small nighttime OH concentrations. Since the available nighttime OH measurements were still under big discussions (e.g., Tan et al., ACP, 2017), we think the nighttime production of HNO_3 from $OH+NO_2$ can be neglected according to the modeled OH concentrations (of about 1×10^5 cm^{-3}). Nevertheless, the unknown nighttime OH chemistry and the possible nighttime produced HNO3 sheds an uncertainty on our current analysis. The impact will be the possible overestimation of the uptake coefficient of N_2O_5 in the current analysis framework. We now extensively discussed the possible influence of the nighttime production of HNO_3 and repartitioning in the revised text as: "The daytime produced HNO_3 will be soon in a new equilibrium with the particulate nitrate within a time scale of about hundred seconds; the nighttime source of HNO_3 are normally negligible except there are significant unknown OH sources at night. Both the gas-particle repartitioning of HNO_3 and nighttime produced HNO_3 will result in the overestimation of γ and underestimation of f."

Reference: Tan, Z., Fuchs, H., Lu, K., Hofzumahaus, A., Bohn, B., Broch, S., Dong, H., Gomm, S., Häseler, R., He, L., Holland, F., Li, X., Liu, Y., Lu, S., Rohrer, F., Shao, M., Wang, B., Wang, M., Wu, Y., Zeng, L., Zhang, Y., Wahner, A., and Zhang, Y.: Radical chemistry at a rural site (Wangdu) in the North China Plain: observation and model calculations of OH, HO_2 and RO_2 radicals, Atmos. Chem. Phys., 17, 663-690, 10.5194/acp-17-663-2017, 2017.

13. L327 "the most rigorous analysis was used in this study". I do not understand what this implies. Most rigorous compared to what?

In Phillips et al., (2016), the first and simplest method is to derive *f* only by using longer time periods (several hours or the whole night) where plots of $ClNO_2$ and NO_3^- are approximately linear. The second method is to calculate absolute production rates of NO_3^- and $ClNO_2$ in shorter periods (1-3 h), when NO_3^- and $ClNO_2$ concentrations both increase during a period of relatively constant composition and environmental variables, such as temperature and RH. In this case, values of $pClNO_2$ and pNO_3^- and average values of S_a and N_2O_5 are used to derive γ and *f*. The last and rigorous method is to avoid the use of the averaged S_a and N_2O_5 in the calculation, the measured N_2O_5, $ClNO_2$, S_a, R, T and NO_3^- were used directly in the calculation in a way of integration (the time step of the calculation were chose to be as small as possible, i.e., the time resolution of the associated measurement parameters). In this study, we used the last method to calculate the N_2O_5 uptake and $ClNO_2$ yield. In the revised manuscript, we changed the description and rewrote this part in line 349 as following: "Based on the observational data of N_2O_5, $ClNO_2$, pNO_3^- and S_a with the time resolution of 5 minutes, the formations of pNO_3^- and $ClNO_2$ were calculated and integrated to reproduce the increasing of pNO_3^- and $ClNO_2$ with estimated values for γ and *f*. The offset of particle nitrate and $ClNO_2$ is the measured particle nitrate and $ClNO_2$ concentration at the start time. The γ and *f* were optimized based on the Levenberg-Marquardt algorithm until good agreement between the observed and predicted concentrations of pNO_3^- and $ClNO_2$ was obtained (Phillips et al., 2016)."

14. L330 Figure 6 would be improved by adding the result of a calculation with lower (factor two?) and higher (factor two?) uptake coefficients to test the sensitivity of the data to the derived parameter. Also, what is the source of the offset in the particle nitrate? How does the particle nitrate look over the diel period? This is essential information when trying to understand the effects of HNO_3 re-partitioning (see comment above).

Thanks for the suggestion, we estimated that the uncertainty of the determined N_2O_5 uptake coefficient was about 55% - 100% (55% shows below as Figure 5), and the scatter of the observed data points could then be explained by the uncertainty of the uptake coefficients. The offset of particle nitrate and $ClNO_2$ is the measured particle nitrate and $ClNO_2$ concentration at the start time point. Normally, the calculation period was the particle nitrate with increasing tendency. We checked the mean diurnal variation of particle nitrate (shows in the Figure A3), which is increased throughout the whole night and continued to the midday. The change of the particulate nitrate is not always follow the re-partitioning due to the temperature

change. Nevertheless, we deduced that the impact of HNO_3 re-partitioning shall be small at night as presented in our answer to comment 12.

Changed in line 351: "The offset of particle nitrate and $ClNO_2$ is the measured particle nitrate and $ClNO_2$ concentration at the start time."

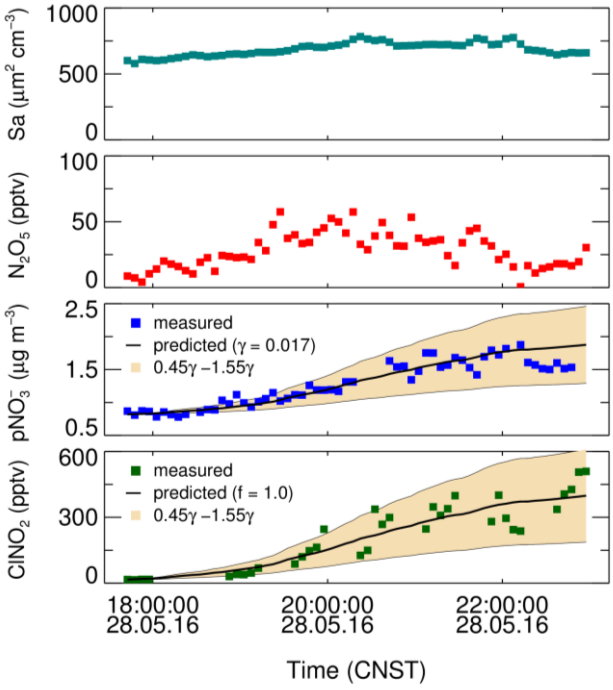

Figure 5. The best fit of γ and f to reproduce the observed $ClNO_2$ and pNO_3^- with an offset on May 28. The black lines are the predicted results of the integrated NO_3^- and $ClNO_2$ by using the observed S_a and N_2O_5.

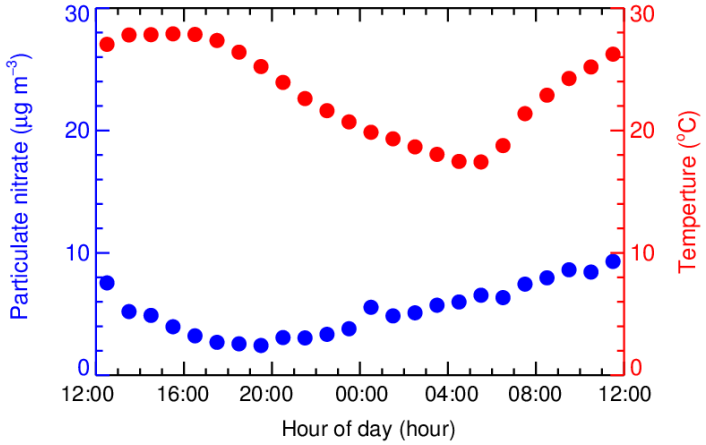

Figure A3. The mean diurnal variation of particulate nitrate during the campaign.

15. L331 "the predicted N_2O_5 uptake coefficient and $ClNO_2$ yield were 0.017 and 1.0, respectively." What are the uncertainties?

The uncertainties added in Table 4, and we added the description: "The uncertainty on each individual fitting is varied from 55% - 100% due to the variability and measurements uncertainties of pNO_3^- and $ClNO_2$."

16. L334 "The errors from each derivation were 30% - 50% and came from the field measurements of S_a, N_2O_5, pNO_3^- and $ClNO_2$." Using the uncertainties listed in Table 1 results in total uncertainty (propagated in quadrature) of > 50 %. I do not understand how the quoted 30-50 % was derived.

As suggested, the propagated uncertainty was added up to 55% according to a Gaussian error propagation approach, here we corrected to "approximately 55%".

17. L369 "The time periods with NO concentration larger than 0.1 ppbv were excluded". Why was this threshold chosen? The lifetime of NO_3 at 0.1 ppbv of NO is about 10-20 s.

The data selection through NO concentrations is based on the assumption that the observed NO smaller than 0.1 ppbv are very small (close to zero). This assumption is plausible as shown by the following analysis. According to a histogram analysis of the observed NO and O_3 concentrations for the conditions of NO smaller than 0.1 ppbv (see the following figure A3), the O_3 concentrations are always larger than 10 ppbv and the NO concentrations are nicely fitting to the Gaussian Distribution, suggesting most of the NO concentration below 0.1 ppbv are instrument noise and the actual value shall be very close to zero. For more rigorous analysis, we constrain the NO concentration of 0.06 ppbv (instrument LOD) in the steady state analysis of the revised text.

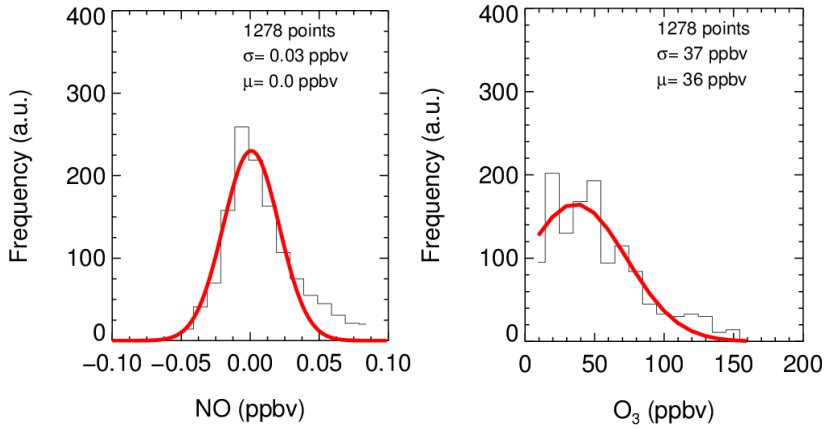

Figure A3. The histogram plot of measured NO concentration below 0.1 ppbv.

Changed line 369: "In this study, the steady state lifetime was only calculated from 20:00 to the next day 04:00. The time periods with NO concentration larger than 0.06 ppbv (instrument LOD) were excluded because the steady state is easily disturbed."

Changed line 378: "The N_2O_5 steady state lifetime ranged from <5 s to 1260 s, with an average of 270 ± 240 s, and large variability was shown during the campaign."

18. L389 the uncertainties in the N_2O_5 loss rate need to be calculated. As this involves NO_2 measurements, the uncertainty will be very large.

Added the following description in the revised text: "Figure 7 shows the time series of the overall N_2O_5 loss rate constant as well as the N_2O_5 steady state loss rate constant. The overall N_2O_5 loss rate constant was calculated from the individual terms (Eq.3). The uncertainties of the N_2O_5 steady state loss rate constant, the overall $k(N_2O_5)$ are estimated to be 67% and 95%, respectively (Eq. 7 and Eq. 8). The largest error sources were from the corrected NO_2 measurements so that it is really important to have accurate NO_2 measurement instrument involved in the future campaigns.

$$\frac{\Delta Lss(N_2O_5)}{Lss(N_2O_5)} = \sqrt{(\frac{\Delta[N_2O_5]}{[N_2O_5]})^2 + (\frac{\Delta[NO_2]}{[NO_2]})^2 + (\frac{\Delta[O_3]}{[O_3]})^2 + (\frac{\Delta K_{eq}}{K_{eq}})^2} \quad \text{(Eq. 7)}$$

$$\frac{\Delta k(N_2O_5)}{k(N_2O_5)} = \sqrt{(\frac{\Delta[N_2O_5]}{[N_2O_5]})^2 + (\frac{\Delta[S_a]}{[S_a]})^2 + (\frac{\Delta[\gamma]}{[\gamma]})^2 + (\frac{\Delta[NO_2]}{[NO_2]})^2 + (\frac{\Delta[O_3]}{[O_3]})^2 + (\frac{\Delta[VOC_s]}{[VOC_s]})^2 + (\frac{\Delta K_{eq}}{K_{eq}})^2} \quad \text{(Eq. 8)."}$$

19. L403 This section deals with oxidation of VOCs and loss of NOx to nitrates (inorganic and organic). NO_3 was not measured but calculated from N_2O_5 and NO_2 (the latter also not measured properly). The NO_3 concentrations derived are therefore

associated with great uncertainty. This needs to be assessed and used in the subsequent discussion and comparison with O_3-induced oxidation.

We carefully performed the uncertainty analysis of the calculated NO_3 concentrations as suggested. We found the uncertainty of calculated NO_3 is 67% associated with the uncertainties of NO_2 and N_2O_5. We also added the following description in the revised text. Added in line 403: "Even the NO_3 concentration in the lower range, NO_3 still responsible for more than 70% nocturnal BVOCs oxidation. The results further confirmed that the oxidation of BVOCs is controlled by NO_3 rather than O_3 in summer Beijing."

20. L416 Similar to k(OH). . .. . . I'm not sure why OH is being mentioned here.

Deleted the "Similar to *k*(OH),".

21. L422 Terpenes were measured using PTRMS, i.e. no speciation. What is the basis for assuming that alpha-pinene can be used as surrogate for NO_3 + terpene reactivity in these air masses?

The speciation measurements of monoterpene are still quite sparse in China. We have now discussed with an expert on this topic. We learnt that the major monoterpene species in Summer Beijing were α-pinene and β-pinene according to GC-MS measurements.

Changed in line 422: "Previous measurement indicated the main detectable monoterpenes were α-pinene and β-pinene in summer Beijing (personal communication with Ying Liu). Here we assumed α-pinene and β-pinene contributes equally to the mixing ratios of the monoterpenes. The average value of the rate coefficients of α-pinene and β-pinene with NO_3 (Atkinson and Arey, 2003) was used as the rate coefficient of monoterpene with NO_3. The uncertainty of the monoterpene + NO_3 rate coefficient in these air masses is thus estimated to be 50%."

22. Figure 9 Needs uncertainties on the two terms being compared.

Thanks for the suggestion, we added the error bar in the Figure 9, the uncertainty of NO_3 calculation initialed by NO_2 was discussed in Question NO. 4

23. Some (certainly not exhaustive) suggestions for improvement of the English. L18 Nocturnal reactive nitrogen compounds play an important role in regional air pollution

Changed accordingly.

24. L27 The concentration of the nitrate radical (NO3) was calculated assuming that. . ..

Changed accordingly.

25. L34 which indicates that reduction of NOx emissions cannot help reduce the nocturnal formation of ONs.

Changed accordingly.

26. L42 NO_3 can initiate the removal of many kind of anthropogenic

Changed accordingly.

27. L58 the reactions of NO_3 with several BVOCs produce considerable amounts of organic nitrates.

Changed accordingly.

28. L207. Nocturnal nitrate radical production rate, P(NO_3), was large, with an average. . .

Changed accordingly.

29. L61 The reaction of NO3 with isoprene has a SOA yield of 23.8% (Ng et al., 2008). For the reaction with a monoterpene, such as limonene, the yield can reach 174% at ambient temperatures (Boyd et al., 2017).

Changed as following; "The reaction of NO_3 with isoprene has a SOA mass yield of 23.8% (Ng et al., 2008). For the reaction with monoterpene, such as limonene, the SOA mass yield can reach 174% at ambient temperatures (Boyd et al., 2017)".

30. L97 the reaction also contributed significantly to NOx.

Changed accordingly.

31. L259 by acid displacement

Changed accordingly.

32. L260 "however, the photolysis with profound $ClNO_2$ was still maintained until noon". I think the authors are trying to say that $ClNO_2$ survived until noon? In this context they should mention the J-values of $ClNO_2$.

Yes, we are trying to say the $ClNO_2$ survived until noon. The campaign average J-values of $ClNO_2$ around noon is about 1.7×10^{-4} s^{-1}. The text changed as following: "However, the $ClNO_2$ can still survive until noon with the averaged daily maximum of $J(ClNO_2)$ to be 1.7×10^{-4} s^{-1}."

33. L273-276. This part needs rewriting. I think the gist if this is that the N_2O_5 concentration depends on the NO_2 level more than on the O_3 concentration. If so, please explain why.

The sentence was rewrote as following: "The N_2O_5 concentration was highly correlated with NO_2 (R^2 = 0.81) and the NO_3 production rate (R^2 = 0.60), suggests the N_2O_5 concentration was solely response to the NO_2 concentration in the background air mass when enough O_3 is presented."

34. L305. Which implies that the $ClNO_2$ formation efficiency.

Changed accordingly.

35. L403 The title of this section is misleading. NO3 is not oxidized, but the VOCs. I suggest "NO3-induced nocturnal oxidation of VOCs" or similar.

Thanks for the suggestion and changed accordingly.

36. L429 for calculating nocturnal ONs production from NO3 oxidation of isoprene and monoterpene, as well as inorganic nitrate production via N2O5 heterogeneous uptake over the same period.

Changed accordingly.

Efficient N_2O_5 Uptake and NO_3 Oxidation in the Outflow of Urban Beijing

Haichao Wang[1], Keding Lu[1*], Song Guo[1], Zhijun Wu[1], Dongjie Shang[1], Zhaofeng Tan[1], Yujue Wang[1], Michael Le Breton[2], Mingjin Tang[3], Yusheng Wu[1], Jing Zheng[1], Limin Zeng[1], Mattias Hallquist[2], Min Hu[1] and Yuanhang Zhang[1,4]

[1]State Key Joint Laboratory or Environmental Simulation and Pollution Control, College of Environmental Sciences and Engineering, Peking University, Beijing, China.

[2]Department of Chemistry and Molecular Biology, University of Gothenburg, Gothenburg, Sweden

[3]State Key Laboratory of Organic Geochemistry and Guangdong Key Laboratory of Environmental Protection and Resources Utilization, Guangzhou Institute of Geochemistry, Chinese Academy of Sciences, Guangzhou, China

[4]CAS Center for Excellence in Regional Atmospheric Environment, Chinese Academy of Sciences, Xiamen, China

**Corresponding to*: Keding Lu (k.lu@pku.edu.cn)

Abstract. Nocturnal reactive nitrogen compounds ~~are~~play an important ~~for understanding~~role in regional air pollution. Here we present the measurements of dinitrogen pentoxide (N_2O_5) associated with nitryl chloride ($ClNO_2$) and particulate nitrate (pNO_3^-) in a suburban site of Beijing in the summer of 2016. High levels of N_2O_5 and $ClNO_2$ were observed in the outflow of the urban Beijing air masses, with 1-min average maxima of 937 pptv and ~~2.9 ppbv~~2900 pptv, respectively. The N_2O_5 uptake coefficients, γ, and $ClNO_2$ yield, f, were experimentally determined from the observed parameters. The N_2O_5 uptake coefficient ranged from 0.012 to 0.055, with an average of 0.034 ± 0.018, which is in the upper range of previous field studies reported in North America and Europe but is a moderate value in the North China Plain (NCP), which reflects efficient N_2O_5 heterogeneous processes in Beijing. The $ClNO_2$ yield exhibited high variability, with a range of 0.50 to unity and an average of 0.73 ± 0.25. The ~~nighttime~~concentration of the nitrate radical (NO_3) was calculated assuming that the thermal equilibrium between NO_3 and N_2O_5 was maintained. In ~~NO_x~~NO_x-rich air masses, the oxidation of nocturnal biogenic volatile organic compounds (BVOCs) was dominated by NO_3 rather than O_3. The production rate of organic nitrates (ONs) via NO_3+BVOCs was significant, with an average of 0.~~11~~10 ± 0.~~09~~07 ppbv h^{-1}. We highlight the importance of NO_3 oxidation of VOCs in the formation of ONs and subsequent secondary organic aerosols in summer in Beijing. The capacities of BVOCs oxidation and ONs formation are maximized and independent of NO_x under a high ~~NO_x~~NO_x/BVOCs ratio condition (>10), which indicates that ~~the initial~~ reduction of ~~the~~ NO_x ~~emission~~emissions cannot help reduce the nocturnal formation of ONs.

带格式的：缩进：首行缩进： 1 字符

带格式的：字体：倾斜，下标

1. Introduction

It has been well recognized that reactive nitrogen compounds, specifically the nitrate radical (NO_3) and dinitrogen pentoxide (N_2O_5), play a key role in nighttime chemistry (Wayne et al., 1991; Brown ~~et al.,~~and Stutz, 2012). NO_3 is the most important oxidant in the nighttime and can be considered the nighttime analogue of the hydroxyl radical (OH) for certain VOCs (Wayne et al., 1991; Benton et al., 2010). NO_3 can initiate the removal ~~processing~~ of many ~~kinds~~kind of anthropogenic and biogenic emissions after sunset. In the ~~NO_x~~NO_x-rich plumes, NO_3 is responsible for the vast majority of the oxidation of biogenic VOCs because of its rapid reactions with unsaturated hydrocarbons (Edwards et al., 2017). NO_3 is predominantly formed by the reaction of NO_2 with O_3 (R1) and further reacts with NO_2 to produce N_2O_5 (R2). Because N_2O_5 is rapidly decomposed back into NO_2 and NO_3 (R3), NO_3 and N_2O_5 are in dynamic equilibrium in the troposphere.

$$NO_2 + O_3 \rightarrow NO_3 + O_2 \quad \text{(R1)}$$

$$NO_2 + NO_3 + M \rightarrow N_2O_5 + M \quad \text{(R2)}$$

$$N_2O_5 + M \rightarrow NO_2 + NO_3 + M \quad \text{(R3)}$$

Photolysis of NO_3 and its reaction with NO are rapid, which leads to a daytime NO_3 lifetime being shorter than 5 s with extremely low concentrations, whereas in low-NO air masses, the fate of NO_3 is mainly controlled by the mixing ratios of various VOCs and N_2O_5 heterogeneous hydrolysis because the two terms are the dominating loss pathways of NO_3 and N_2O_5. The VOCs reaction is significant downwind of ~~a~~an urban area or a strongly urban-influenced forested area in summer. The NO_3 oxidation of VOCs was responsible for more than 70% nocturnal NO_3 loss in Houston (Stutz et al., 2010) and contributed approximately 50% in the forest region in Germany (Geyer et al., 2001). The reactions of NO_3 with several BVOCs produce considerable amounts of organic nitrates (ONs) with efficient yields, which act as important precursors of secondary organic aerosols (SOA). The reaction of NO_3 with isoprene has a ~~considerable~~ SOA mass yield of 23.8% (Ng et al., 2008~~), and~~). For the reaction with monoterpene, such as limonene, the SOA mass yield can reach 174% at ambient temperatures (Boyd et al., 2017). The reactions of NO_3+BVOCs are critical to the studies of aerosols on regional and global scales (Fry et al., 2009; Rollins et al., 2009; Pye et al., 2010; Ng et al., 2017). For example, ONs had extensive percentages of fine particulate nitrate (pNO_3^-) (34% - 44%) in Europe (Kiendler-Scharr et al., 2016).

The heterogeneous hydrolysis of N_2O_5 produces soluble nitrate (HNO_3 or NO_3^-) and nitryl chloride ($ClNO_2$) on chloride-containing aerosols (R4) (Finlayson-Pitts et al., 1989). This reaction is known to be an important intermediate in the ~~NO_x~~NO_x removal processes (Brown et al., 2006). The pseudo-first order loss rate ~~coefficient of the~~constant N_2O_5 via heterogeneous ~~N_2O_5 reaction~~uptake is given in Eq. 1 (~~Tang~~Wahner et al., ~~2017~~1998).

$$N_2O_5 + (H_2O \text{ or } Cl^-) \rightarrow (2 - f)\, NO_3^- + f\, ClNO_2 \quad \text{(R4)}$$

$$k_{N2O5} = 0.25 \cdot c \cdot \gamma(N_2O_5) \cdot S_a \quad \text{(Eq. 1)}$$

~~where~~Where c is the mean molecule speed of N_2O_5, S_a is the aerosol surface concentration and $\gamma(N_2O_5)$ is the N_2O_5 uptake coefficient. N_2O_5 heterogeneous hydrolysis is one of the major uncertainties of the NO_3 budget since the N_2O_5 uptake coefficient can be highly variable and difficult to quantify (Brown and Stutz, 2012; Chang et al., 2011; H. C. Wang et al., 2016). Laboratory and field measurement studies have reported that the N_2O_5 uptake coefficient has large variability and ranges from <0.001 to 0.1; the N_2O_5 uptake coefficient is subject to relative humidity (RH), particle morphology, compositions (water content, nitrate, sulfate, organic or mineral particles) and other factors (e.g., Wahner et al., 1998; Mentel et al., 1999; Hallquist et al., 2003; Thornton et al., 2003; Thornton et al., 2005; Brown et al., 2006; Bertram and Thornton, 2009; Tang et al., 2012, 2014; Gaston et al., 2014; Grzinic et al., 2015). The coupled chemical mechanisms in ambient conditions are still not well understood. $ClNO_2$ forms and accumulates with a negligible sink during the night and further ~~photolyzes~~photolysis and liberates the chlorine radical (Cl) and NO_2 after sunrise. Hundreds of pptv to ppbv of $ClNO_2$ can lead to several ppbv of O_3 enhancement and significant primary RO_x production (Osthoff et al., 2008; Thornton et al., 2010; McLaren et al., 2010; Riedel et al., 2014; Sarwar et al., 2014; Tham et al., 2016).

Large amounts of ~~NO_x~~NO_x have been emitted for the past several decades in China, but comprehensive field studies of the nighttime chemical processes of reactive nitrogen oxides remain sparse. Previous studies have found high mixing ratios of NO_3 associated with high NO_3 reactivity in the megacities in China, including Shanghai, the Pearl River Delta (PRD) and Beijing (Li et al., 2012; Wang et al., 2013; Wang et al., 2015). N_2O_5 concentration was elevated in Beijing (H. C. Wang et al., 2017a; H. C. Wang et al., 2017c) but was moderate in other places of North China Plain (NCP), such as Wangdu, Jinan and Mount Tai (Tham et al., 2016; X. F. Wang et al., 2017; Z. Wang et al., 2017). Recently, the N_2O_5 uptake coefficients were determined to be very high, even up to 0.1 in NCP, but the reason is still not well studied (H. C. Wang et al., 2017c; X. F. Wang et al., 2017; Z. Wang et al., 2017). Reactive N_2O_5 chemistry was also reported in Hong Kong, ~~which had~~and showed the highest field-observed N_2O_5 concentration to date (T. Wang et al., 2016; Brown et al., 2016). Observations and model simulations revealed that fast heterogeneous uptake of N_2O_5 is an important pathway of pNO_3^- formation in China (H. C. Wang et al., 2017b; H. C. Wang et al., 2017c; Z. Wang et al., 2017; Su et al., 2017); the reaction also ~~considerably~~ contributed significantly to ~~NO_x~~-removal (Z. Wang et al., 2017; Brown et al., 2016). Moreover, chlorine activation from N_2O_5 uptake had a significant effect on daytime photolysis chemistry in China (Xue et al., 2015; Li et al., 2016; Tham et al., 2016; T. Wang et al., 2016).

In this study, to quantify the contribution of NO_3 and N_2O_5 chemistry to the atmospheric oxidation capacity and the ~~NO_x~~NO_x removal process in the outflow of urban Beijing, we reported the measurement of N_2O_5, $ClNO_2$, and related species in the surface layer of a suburban site in Beijing and determined the N_2O_5 heterogeneous uptake coefficients and $ClNO_2$ yields. The nighttime NO_3 oxidation of biogenic VOCs and its impact on the ONs formation in the ~~NO_x~~NO_x-rich region were diagnosed. Finally, the nighttime ~~NO_x~~NO_x removal via the NO_3 and N_2O_5 chemistry was estimated and discussed.

2. Method

2.1 The site

带格式的：字体：非倾斜

带格式的：字体：倾斜，下标

Within the framework of a Sino-Sweden joint research project, "Photochemical Smog in China", a summer field campaign was conducted in Beijing to enhance our understanding of the secondary chemistry via photochemical smog and the heterogeneous reactions (Hallquist et al., 2016). The data presented here were collected at a regional site, PKU-CP (Peking University Changping campus), from 23 May to 5 June 2016. The measurement site is located in the northern rural area of Beijing, approximately 45 km from the city center; the closest road is approximately 1 km to the south, and there are no major industry surroundings (Figure. 1). The site is surrounded to the north, east and west by mountains. The general feature of this site is that it captures air masses with strong influences from both urban and biogenic emissions. Instruments were set up on the fifth floor of the main building of the campus with inlets approximately 12 m above the ground. Time is given in this paper as CNST (Chinese National Standard Time = UTC+8 h). During the campaign, sunrise was at 05:00 CNST and sunset was at 19:30 CNST.

2.2 Instrument setup

A comprehensive suite of trace gas compounds and aerosol properties was measured in the field study, and the details are listed in Table 1. N_2O_5 was measured by a newly developed cavity enhanced absorption spectrometer (CEAS; H. C. Wang et al., 2017a). In the CEAS, ambient N_2O_5 was thermally decomposed to NO_3 in a perfluoroalkoxy alkanes (PFA) tube (length: 35 cm, I.D.: 4.35 mm) heated to 120 °C and was then detected within a PFA resonator cavity; the cavity was heated to 80 °C to prevent NO_3 reacting back to N_2O_5. Ambient gas was sampled with a 1.5-m sampling line (I.D.: 4.35 mm) with a flow rate of 2.0 L min^{-1}. NO was injected for 20 seconds to destroy NO_3 from N_2O_5 thermal decomposition in a 5-minute cycle, and the corresponding measurements were then used as reference spectra ~~(I_0).~~. A Teflon polytetrafluoroethylene (PTFE) filter was used in the front of the sampling module to remove ambient aerosol particles. The filter was replaced with a fresh one every hour to avoid the decrease of N_2O_5 transmission efficiency due to aerosol accumulation on the filter. The limit of detection (LOD) was 2.7 pptv (1σ), and the measurement uncertainty was 19%.

$ClNO_2$ and N_2O_5 were also detected using a Time of Flight Chemical Ionization Mass Spectrometer (ToF-CIMS) with the Filter Inlet for Gas and AEROsols (FIGAERO; Lopez-Hilfiker et al., 2014; Bannan et al., 2015). Briefly, the gas phase species were measured via a 2-m-long, 6-mm-outer-diameter PFA inlet while the particles were simultaneously collected on a Teflon filter via a separate 2-m-long, 10-mm-outer-diameter copper tubing inlet; both had flow rates of 2 L min^{-1}. The gas phase was measured for 25 minutes at 1 Hz, and the FIGAERO instrument was then switched to place the filter in front of the ion molecule region; it was then heated incrementally to 200 °C to desorb all the mass from the filter to be measured in the gas phase, which resulted in high-resolution thermo grams. Formic acid calibrations were performed daily using a permeation source maintained at 40 °C. Post-campaign laboratory calibrations of N_2O_5 were first normalized to the campaign formic acid calibrations to account for any change in sensitivity (Le Breton et al., 2014). Then, $ClNO_2$ measurements were quantified by passing the N_2O_5 over a wetted NaCl bed to produce $ClNO_2$. The decrease in N_2O_5 from the reaction with NaCl was assumed to be equal to the concentration of $ClNO_2$ produced (i.e., 100% yield). The sensitivities of the CIMS to N_2O_5 and $ClNO_2$ were found to be 9.5 and 1.2 ion counts per pptv Hz^{-1}, respectively, with errors of 23% and 25% for $ClNO_2$ and N_2O_5, respectively. The ~~limit of detection (~~LOD~~)~~ for $ClNO_2$ and N_2O_5 were 16 and 8 pptv, respectively. An

intercomparison of N_2O_5 measurements between the CEAS and FIGAERO-ToF-CIMS showed good agreement; a companion paper on chlorine photochemical activation during this campaign gives detailed intercomparison results of N_2O_5 measured by the two different techniques (Le Breton et al., 2018).

Sub-micron aerosol composition ($PM_{1.0}$), including nitrate, sulfate, chloride, ammonium and organic compounds, were measured by a High Resolution Time of Flight Aerosol Mass Spectrometer (HR-ToF-AMS) (~~DeCarlo~~De Carlo et al, 2006, Zheng et al., 2017). Particle number and size distribution (PNSD) was measured by a scanning mobility particle sizer (SMPS, TSI 3936) and an aerosol particle sizer (APS, TSI 3321) (Yue et al., 2009). SMPS measured the particles in the range between 3.5 nm and 523.3 nm in diameter, and APS measured the particles with a diameter range from 597.6 nm to 10.0 μm. S_a was calculated based on the dry-state particle number and geometric diameter in each size bin (3.5 nm - 2.5 μm). Dry-state S_a was corrected to wet particle-state S_a for particle hygroscopicity by a growth factor. The growth factor, $f(RH)=1 + 8.77 \times (RH/100)^{9.74}$, was derived from the measurement of aerosol extinction as a function of RH in autumn in Beijing and is valid for 30% < RH < 90% (Liu et al., 2013). The uncertainty of the wet aerosol surface areas was estimated to be ~30%, associated from the error from dry PNSD measurement (~20%) and the growth factor (~20%). During this measurement, fine particles below 500 nm contributed to more than 90% of the total ~~particle aerosol surface area~~S_a.

VOCs were measured by Proton Transfer Reaction Mass Spectrometry (PTR-MS) with a time resolution of 5 minutes (de Gouw and Warneke et al., 2007; Wang et al., 2014). A commercial instrument (Thermo Electron model 42i) equipped with a molybdenum-catalytic converter was used to monitor ~~NO_x~~NO_x. The LODs were 60 pptv (1 min) for NO and 300 pptv (1 min) for NO_2, with both at a 20% precision (Tan et al., 2017). The molybdenum-catalytic technique not only converts NO_2 to NO but also converts ambient NO_y such as peroxyacetyl nitrate (PAN) and HNO_3. Therefore, the measured NO_2 concentration corresponded to $NO_2 + NO_y$ and was normally higher than the real concentration, especially in an aged air mass with high NO_x conditions. In this study, we used a factor of 0.6 to correct the nighttime NO_2 concentration (a detailed explanation is in the Support Information Text S1 and Figure S1). The correction factor (0.6) used to be the averaged scaled value of the correction factors during nighttime, the standard deviation of the daytime correction factor for all the air masses experienced at Changping site was determined to be 0.27 (1σ), which extended to nighttime and result in an uncertainty of correction to be 45%. The uncertainty of NO_2 is therefore about 50% when further included the associated measurement uncertainty from calibrations. O_3 was measured by a commercial instrument using ultraviolet (UV) absorption (Thermo Electron model 49i); the LOD was 0.5 ppbv, with an uncertainty of 5%. The mass concentration of $PM_{2.5}$ was measured using a standard Tapered Element Oscillating Microbalance (TEOM, 1400A analyzer). Meteorological parameters included relative humidity, temperature, pressure, wind speed, and wind direction and were available during the campaign. Photolysis frequencies were calculated from the spectral actinic photon flux density measured by a spectroradiometer (Bohn et al., 2008).

带格式的：字体：倾斜

带格式的：字体：倾斜

3. Results

3.1 Overview

During the campaign, the meteorological conditions of the site ~~were characterized by~~was high temperature and low relative humidity (RH); the temperature ranged from 10 - 34 °C and was 23 ± 5 °C on average, and RH ranged from 10% - 80%, with an average of 37% ± 15%. Because of the special terrain of the observation site, the local wind was measured by the in situ meteorological stations; the site has a typical mountain-valley breeze that cannot reflect the general air mass movement patterns at slightly higher altitudes. Figure ~~2~~S2 shows the calculated backward trajectories using the Hybrid Single-Particle Lagrangian Integrated Trajectory (HYSPLIT) model (Draxler and Rolph, 2003); these images show the 24-h backward particle dispersion trajectories for 12:00 local time (CNST) as the starting time during May 23 - July 5, 2016. According to the results of HYSPLIT, the arrivals of air masses were mainly from the northwest and the south. Therefore, we meteorologically separated the measurement period into two parts. The first three days show that the air masses came from the north or northwest; the air masses represent the background region (defined as Background Air Mass, BAM). The air masses after May 26 originated from the polluted NCP and passed over urban Beijing; they were characterized by large ~~NO$_x$~~NO_x emissions and severe photochemical pollution (defined as Urban Air Mass, UAM).

The time series of N_2O_5, $ClNO_2$ and other relevant species are shown in Figure ~~3~~2, and nighttime statistical results are listed in Table S1. The daily 8-h maximum of O_3 concentration exceeded 93 ppbv (Chinese national air quality standard) for 8 of 12 days, and all the O_3-polluted air masses came from the urban region. When the air masses were from the background region, the daily maximum of O_3 was only approximately 60 ppbv, much lower than that from the urban region. The NO_2 concentration was elevated, with a nocturnal average value over 10 ppbv during the urban air mass period. The nocturnal nitrate radical production rate, $P(NO_3)$, was ~~significant~~large, with an average of 1.2 ± 0.9 ppbv h^{-1}, which is comparable with rates previously reported in the NCP and Hong Kong (Tham et al., 2016; Brown et al., 2016; Z. Wang et al., 2017; X. F. Wang et al., 2017). The daily peaks of N_2O_5 were 100-500 pptv most nights; the maximum of 937 pptv in a 1-min average was observed near 20:00 on the early night of June 2, when the $P(NO_3)$ was up to 4 ppbv h^{-1}. The average mixing ratio of N_2O_5 was 73 ± 90 pptv, which is much higher than recent measurements reported in North China (Tham et al., 2016; X. F Wang et al., 2017; Z. Wang et al., 2017) but much lower than that observed in the residual layer of the outflow from the PRD region, where the N_2O_5 was up to 7.7 ppbv (T. Wang et al., 2016). With an elevated O_3 mixing ratio in the first half of the night, the NO lifetime was only several minutes, and the mixing ratio of NO concentration was observed below the detection limit. During the second half of the night when the O_3 concentration was consumed to low concentration, high levels of NO could occasionally be observed, and N_2O_5 dropped to zero because of the fast titration by NO, such as the events that occurred on the second half of the nights of May 24, 28, 30. The $PM_{2.5}$ mass concentration was moderate during the measurement period, with an average of 26 ± 21 μg m^{-3}, and the average aerosol surface area was 560 ± 340 μm^2 cm^{-3}. Elevated $ClNO_2$ was observed to have a daily maximum 1-min average of over 800 pptv during the urban air masses period; the campaign maximum of up to ~~2.9 ppbv~~2900 pptv was observed on the morning (05:30) of May 31, which implied that fast N_2O_5 heterogeneous hydrolysis and effective $ClNO_2$ yields are common in Beijing. The level of $ClNO_2$ was comparable with the results in NCP (Tham et al., 2016; X. Wang et al., 2017; Z. Wang

带格式的: fontstyle01

et al., 2017) but slightly higher than that measured in coastal (e.g., Osthoff et al., 2008) and inland sites (e.g., Thornton et al., 2010) in other regions of the world.

3. 2 Mean diurnal profiles

The mean diurnal profiles of the measured NO_2, O_3, N_2O_5, $ClNO_2$ and the particle chloride content are shown in Figure ~~4~~3, as well as the calculated NO_3 based on the thermal equilibrium of NO_2, NO_3 and N_2O_5. The left ~~panels~~panel show the average results of the BAM period, and the right panels show those of the UAM period. The NO_2 and O_3 from the UAM were much higher than were those from the BAM, as were the mixing ratios of N_2O_5, NO_3 and $ClNO_2$. The daily variation tendencies of those species in the two kinds of air masses were similar. N_2O_5 began to accumulate in the late afternoon and increased sharply after sunset. ~~The single~~A peak occurred near 20:00 and ~~then gradually~~ decreased ~~to~~below the ~~LOD before~~instrument detection limit at sunrise; the N_2O_5 maxima occurred at a similar time to our previous observation in urban Beijing (H. C. Wang et al., 2017c); however, the N_2O_5 decrease rate after the peak time was much slower than that in urban Beijing, where the N_2O_5 dropped to almost zero in 2-4 hours, which suggests a relatively slow N_2O_5 loss rate in suburban Beijing. The daily average peaks of N_2O_5 during the BAM period and the UAM period were approximately 75 pptv and 150 pptv, respectively. The calculated NO_3 diurnal profile was quite similar to that of N_2O_5, and the daily average peaks of NO_3 during the BAM and UAM periods were approximately 11 pptv and 27 pptv, respectively. The uncertainty of NO_3 calculation was estimated to be 67% according to Eq. 2 which is dominated by uncertainty of the NO_2 concentrations

~~$ClNO_2$ accumulated corresponding to N_2O_5 after sunset but $ClNO_2$ peaked in the middle or the second half of the night since the nocturnal sinks of $ClNO_2$ were negligible to our knowledge.~~ $\frac{\Delta[NO_3]}{[NO_3]} = \sqrt{(\frac{\Delta[N_2O_5]}{[N_2O_5]})^2+(\frac{\Delta[NO_2]}{[NO_2]})^2 + (\frac{\Delta[O_3]}{[O_3]})^2 + (\frac{\Delta K_{eq}}{K_{eq}})^2}$ (Eq. 2)

The observed $ClNO_2$ concentrations showed a clear increase after sunset and reached a maximum before sunrise for BAM period while reached a maximum around midnight for the UAM period. The diurnal peak of $ClNO_2$ in the BAM period was approximately 125 pptv, whereas the diurnal peak of $ClNO_2$ was over 780 pptv in the UAM period and approximately 6 times as high as that in the UAM period. Particle chloride (Cl^-) is regarded as a key factor that affected the $ClNO_2$ yield on aerosol surface. Higher particle chloride led to higher $ClNO_2$ yield and promoted the N_2O_5 conversion to $ClNO_2$ (e.g., ~~Roberts~~Finlayson-Pitts et al., ~~2009~~1989; Behnke et al., 1997), whereas the particle chloride content during the measurement was below 60 pptv and was much lower than the mixing ratio of $ClNO_2$. The HYSPLIT model results showed that the air masses had almost always continental conditions; as was mentioned above, fine particles dominated the S_a, which meant that large amounts of the particle chloride were not replenished by NaCl from marine sources but possibly by gas-phase HCl (Ye et al., 2016). Cl^- was found to be correlated strongly with CO and SO_2, likely to originate from an anthropogenic source, such as power plants or combustion sources (Le Breton et al., 2018). ~~Up~~The required nocturnal source of Cl^- to support the $ClNO_2$ production is further estimated through

带格式的: 默认段落字体，字体颜色：文字 1

its loss rate. The $\gamma \times f$ was set to the campaign average value (0.019) (see Sect. 4.1), and real-time Cl^- loss rate via N_2O_5 can be calculated based on the measured N_2O_5 and S_a by Eq.3.

$$L[Cl^-] = (\gamma \times f) \cdot \int_{t_{sunset}}^{t_{sunrise}} \frac{C \cdot S_a}{4} [N_2O_5] dt \qquad \text{(Eq. 3)}$$

Here the $L(Cl^-)$ denotes the integral Cl^- loss to form the $ClNO_2$ per night. The required source term of the Cl^- need to support the $ClNO_2$ formation during the campaign was range from (0.5 - 4.0 ppbv per night) with (1.7 ± 2.3 ppbv per night) on average. The gas phase HCl predicted by the ISORROPIA II model showed that the HCl concentration near sunset period was high enough (much larger than 2 ppbv) to support the $ClNO_2$ formation (Figure. S3). Note that up to 10 ppbv of HCl was observed ~~by a Gas and Aerosol Collector combined with Ion Chromatography (GAC-IC; Dong et al., 2012)~~ in the urban Beijing in September, 2016, ~~which implies~~we believe that the potential particle Cl^- source was sufficient and gas-phase HCl was possibly the main particle chloride source by the acid ~~replacement~~displacement reaction. After sunrise, $ClNO_2$ was photolyzed and decreased with the increasing photolysis intensity; ~~however~~However, the ~~photolysis with profound~~ ClNO2 ~~was~~can still ~~maintained~~survive until noon~~.~~ with the averaged daily maximum of $J(ClNO_2)$ to be 1.7×10^{-4} s^{-1}. Similar to the studies reported in London, Texas and Wangdu (Bannan et al., 2015; Faxon et al., 2015; Tham et al., 2016), we observed sustained elevated $ClNO_2$ events after sunrise in 5 of 12 days. For example, on the morning of May 30, $ClNO_2$ increased after sunrise and peaked at approximately 8:00 am, with a concentration over 500 pptv, which was impossible from the local chemical formation since N_2O_5 dropped to almost zero and the needed N_2O_5 uptake coefficients were unrealistically high. Previous work has suggested that abundant $ClNO_2$ produced in the residual layer at night and downward transportation in the morning may help to explain this phenomenon (Tham et al., 2016).

3.3 Variation of N_2O_5 in the background air masses

During the BAM period, the O_3 concentration was well in excess of NO_2. In the NO_3 and N_2O_5 formation processes, the limited NO_2 in high O_3 region indicates that the variation of NO_2 is more essential to the variation of the N_2O_5 concentration. As shown in Figure ~~5~~4, during the night of May 24 (20:00 - 04:00), the local emission of NO was negligible. O_3 concentration was larger than 25 ppbv, much higher than NO_2 and free of the local NO emission. The ~~variation of~~ N2O5 concentration was highly correlated with ~~the mixing ratio of~~ NO2 (R2 = 0.81~~). The result suggests that when the air mass with high O_3 was sampled from the background air mass, the N_2O_5 concentration was especially dependent on the NO_2 concentration rather than O_3. Furthermore, The variation of N_2O_5 concentration was strongly correlated with~~) and the NO3 production rate (R2 = 0.60), ~~suggesting~~suggests the ~~mixing ratio of~~ N2O5 concentration was ~~subject~~solely response to the ~~formation processes~~ NO_2 concentration in ~~clean air masses.~~the background air mass when enough O_3 is presented.

3.4 Elevated $ClNO_2$ to N_2O_5 ratio

带格式的：缩进：首行缩进： 0 字符，定义网格后自动调整右缩进，段落间距段前：0 磅，段后：0.5 行，到齐到网格，图案：清除（白色）
带格式的：默认段落字体，字体颜色：文字 1
带格式的：默认段落字体，字体颜色：文字 1
带格式的：默认段落字体，字体颜色：文字 1，非上标/ 下标
带格式的：默认段落字体，字体颜色：文字 1
带格式的：默认段落字体，字体颜色：文字 1
带格式的：默认段落字体，字体颜色：文字 1
带格式的：字体颜色：蓝色
带格式的：默认段落字体，字体颜色：文字 1
带格式的：默认段落字体，字体颜色：文字 1
带格式的：默认段落字体，字体颜色：文字 1，非上标/ 下标
带格式的：默认段落字体，字体颜色：文字 1
带格式的：默认段落字体，字体颜色：文字 1，非上标/ 下标
带格式的：默认段落字体，字体颜色：文字 1
带格式的：默认段落字体，字体颜色：文字 1
带格式的：默认段落字体，字体颜色：文字 1，非上标/ 下标
带格式的：默认段落字体，字体颜色：文字 1
带格式的：默认段落字体，字体颜色：文字 1，非上标/ 下标
带格式的：默认段落字体，字体颜色：文字 1
带格式的：默认段落字体，字体颜色：文字 1
带格式的：默认段落字体，字体颜色：文字 1，非上标/ 下标
带格式的：默认段落字体，字体颜色：文字 1
带格式的：默认段落字体，字体颜色：文字 1，非上标/ 下标
带格式的：默认段落字体，字体颜色：文字 1
带格式的：默认段落字体，字体颜色：文字 1
带格式的：默认段落字体，字体颜色：文字 1
带格式的：默认段落字体，字体颜色：文字 1，非上标/ 下标
带格式的：默认段落字体，字体颜色：文字 1
带格式的：默认段落字体，字体颜色：文字 1，非上标/ 下标
带格式的：默认段落字体，字体颜色：文字 1
带格式的：默认段落字体，字体颜色：文字 1
带格式的：默认段落字体，字体颜色：文字 1
带格式的：默认段落字体，字体颜色：文字 1

Large day-to-day variabilities of N_2O_5 and $ClNO_2$ were observed during the measurement period. Following the work of Osthoff et al. (2008), Mielke et al. (2013), Phillips et al. (2012) and Bannan et al. (2015), we used the ~~relative production rates,~~concentration ratio of $ClNO_2$~~:~~ to N_2O_5, to describe the conversion capacity of N_2O_5 to $ClNO_2$. The nighttime peak values and mean values of $ClNO_2$: N_2O_5 were used to calculate the ratios~~, and two kinds of daily ratios~~ are listed in Table S2, the calculation period is from 19:30 to the next day 05:00. The average nighttime ratio ranged from 0.7 to 42.0, with a mean of 7.7 and a median of 6.0. The $ClNO_2$ formation was effective, with $ClNO_2$:N_2O_5 ratios larger than 1:1 throughout the campaign, except for the night of May 26, when the ratio was 0.7:1. Previous observations of the $ClNO_2$:N_2O_5 ratios are summarized in Table 2. Compared with the results conducted in similar continental regions in Europe and America (0.2 - 3.0), the ratios in this work were significantly higher and consistent with the recent studies in the NCP~~,~~ (Tham et al., 2016; X. F. Wang et al., 2017; Z. Wang et al., 2017), which suggests that high $ClNO_2$: N_2O_5 ratios were ubiquitous in the NCP and implies that the $ClNO_2$ yield via N_2O_5 uptake is efficient.

4. Discussion

4.1 Determination of N_2O_5 uptake coefficients

A composite term, $\gamma \times f$, was used to evaluate the ~~overall $ClNO_2$ yield from N_2O_5 heterogeneous hydrolysis (Mielke et al., 2013); the term was estimated by considering the production rate of $ClNO_2$ and using the measured N_2O_5 and S_a. The values calculated based on the field observations are listed in Table S3 and~~production of $ClNO_2$ from N_2O_5 heterogeneous hydrolysis (Mielke et al., 2013). $\gamma \times f$ was estimated by fitting the observed $ClNO_2$ in a time period when the nighttime concentrations of $ClNO_2$ kept increasing. The increased $ClNO_2$ was assumed to be solely from the N_2O_5 uptake. The fitting was optimized by changing the input of $\gamma \times f$ associated with the measured N_2O_5 and S_a, until the $ClNO_2$ increasing was well reproduced (Eq. 4). Here t_0 and t denote the start time and end time, respectively, $[ClNO_2](t_0)$ is the observed concentration at t_0 and set as the fitting offset. The calculation time duration was normally several hours, and the derived $\gamma \times f$ was found to be constant with small uncertainties for optimization (see Table S3). It is worth to be noticed that both the N_2O_5 and S_a is not necessary to be stable in this calculation due to the use of integration.

$$[ClNO_2](t) = [ClNO_2](t_0) + (\gamma \times f) \cdot \int_{t_0}^{t} \frac{C \cdot S_a}{4} [N_2O_5]\,dt \qquad \text{(Eq. 4)}$$

The values of $\gamma \times f$ had moderate variability, a range from 0.008 - 0.035 and an average of 0.019 ± 0.009. Table 3 summarizes the $\gamma \times f$ values derived in the previous field observations. The value in suburban Germany was between 0.001 and 0.09, with the average of 0.014 (Phillips et al., 2016), and the average value in Mt. Tai, China, was approximately 0.016 (Z. Wang ~~X~~ et al., 2017). Therefore, the average value in this study was comparable with that of the two suburban sites, whereas in an urban site of Jinan, China~~,~~ (X. F. Wang et al., 2017), the value was lower than 0.008 and comparable with that in the CalNex-LA campaign. The three sets of $\gamma \times f$ values from suburban regions were approximately twice as large as those in urban regions, which implies that the ~~composited~~ $ClNO_2$ ~~yields~~formation efficiency in the aged air masses in suburban regions were more efficient than in the

urban region. The difference of the overall yield between the two regions may have been caused by (1) the particle morphology variation because of particle aging, such as the particle mixing state, O: C ratio, particle viscosity and solubility (Riemer et al., 2009; Gaston et al., 2014; Grzinic et al., 2015) or (2) the particle compound variation such as the liquid water content and the Cl^- content. The liquid water content and the Cl^- content were proposed to affect the $ClNO_2$ yield because those particle physicochemical properties were reported to affect the N_2O_5 uptake coefficient (Bertram and Thornton, 2009).

According to reaction R4, pNO_3^- and $ClNO_2$ were formed by N_2O_5 heterogeneous uptake, with yields of 2 - *f* and *f*, respectively. Following the recent work of Phillips et al., (2016), we used the observed pNO_3^- and $ClNO_2$ formation rates to derive individual γ and *f*. The calculations assumed that the relevant properties of the air mass are conserved and that the losses of produced species are negligible; additionally, the N_2O_5 uptake coefficients and the $ClNO_2$ yield are independent of particle size. The nights characterized by the following two features were chosen for further analysis: (1) ~~A clear covariance existed~~for some nights, significant correlations between ~~the pNO_3^- and $ClNO_2$, which indicated that~~ pNO3- and ClNO2 were ~~to some extent predominantly produced by N_2O_5 uptake, and~~presented ($R^2 > 0.5$); while on the other nights, the ~~HNO_3 uptake was~~R^2 were always smaller than 0.2, which is not ~~important for pNO_3^- formation~~meet the theoretical hypothesis of this method. In this case, we chose the nights with high correlations. (2) An equivalent or increase in ammonium was accompanied by an increase of pNO_3^-, which suggested that the gas-phase ammonia was repartitioned to form ammonium nitrate and suppress the release of HNO_3. The rich-ammonia conditions in Beijing (Liu et al., 2017) demonstrated that the degassing of HNO_3 at night can be effectively buffered by the high concentrations of ammonia presented in the NCP. For the nocturnal HNO_3 uptake effect, the daytime produced HNO_3 will be soon in a new equilibrium with the particulate nitrate within a time scale of about hundred seconds; the nighttime source of HNO_3 are normally negligible except there are significant unknown OH sources at night. Both the gas-particle repartitioning of HNO_3 and nighttime produced HNO_3 will result in the overestimation of γ and underestimation of *f*. During this campaign, five nights were eligible for the following analysis. ~~Three different types of derivation were proposed by Phillips et al., (2016), based~~Based on the observational data of N2O5, ClNO2, pNO3- and Sa~~; the most rigorous analysis was used in this study. The~~ with the time resolution of 5 minutes, the formations of pNO3- and ClNO2 were calculated and integrated ~~based on~~to reproduce the ~~measured S_a~~increasing of pNO_3^- and ~~N_2O_5 from 5-min-averaged datasets and an~~$ClNO_2$ with estimated ~~initial γ and *f*.~~ values for γ and *f*. The offset of particle nitrate and $ClNO_2$ is the measured particle nitrate and $ClNO_2$ concentration at the start time. The γ and f were optimized based on the Levenberg-Marquardt algorithm until good agreement between the observed and predicted concentrations of pNO3- and ClNO2 was obtained~~.~~ (Phillips et al., 2016). Figure ~~6~~5 depicts an example of the fitting results on May 28, the predicted N_2O_5 uptake coefficient and $ClNO_2$ yield were 0.017 and 1.0, respectively. The uncertainty on each individual fitting is varied from 55% - 100% due to the variability and measurements uncertainties of pNO_3^- and $ClNO_2$. Five sets of values of γ and *f* obtained are listed in Table 4. N_2O_5 uptake coefficients ranged from 0.012 - 0.055, with an average of 0.034 ± 0.018, and the $ClNO_2$ yield ranged from 0.50 to unity, with an average of 0.73 ± 0.25. The errors from each derivation were ~~30% - 50~~about approximately 55% and came from the field measurements of S_a, N_2O_5, pNO_3^- and $ClNO_2$.

带格式的：默认段落字体，字体颜色：文字 1
带格式的：默认段落字体，字体颜色：文字 1
带格式的：默认段落字体，字体颜色：文字 1，非上标/ 下标
带格式的：默认段落字体，字体颜色：文字 1
带格式的：默认段落字体，字体颜色：文字 1，非上标/ 下标
带格式的：默认段落字体，字体颜色：文字 1
带格式的：默认段落字体，字体颜色：文字 1
带格式的：默认段落字体，字体颜色：文字 1
带格式的：默认段落字体，字体颜色：文字 1
带格式的：默认段落字体，字体颜色：文字 1
带格式的：默认段落字体，字体颜色：文字 1，非上标/ 下标
带格式的：默认段落字体，字体颜色：文字 1
带格式的：默认段落字体，字体颜色：文字 1，非上标/ 下标
带格式的：默认段落字体，字体颜色：文字 1
带格式的：默认段落字体，字体颜色：文字 1，非上标/ 下标
带格式的：默认段落字体，字体颜色：文字 1
带格式的：默认段落字体，字体颜色：文字 1，非上标/ 下标
带格式的：默认段落字体，字体颜色：文字 1
带格式的：默认段落字体，字体：非倾斜，字体颜色：文字 1
带格式的：默认段落字体，字体：非倾斜，字体颜色：文字 1，非上标/ 下标
带格式的：默认段落字体，字体颜色：文字 1
带格式的：默认段落字体，字体颜色：文字 1，非上标/ 下标
带格式的：默认段落字体，字体颜色：文字 1
带格式的：默认段落字体，字体颜色：文字 1，非上标/ 下标
带格式的：默认段落字体，字体颜色：文字 1
带格式的：默认段落字体，字体颜色：文字 1
带格式的：默认段落字体，字体颜色：文字 1
带格式的：默认段落字体，字体颜色：文字 1
带格式的：默认段落字体，字体颜色：文字 1
带格式的：默认段落字体，字体：非倾斜，字体颜色：文字 1
带格式的：默认段落字体，字体颜色：文字 1
带格式的：默认段落字体，字体：非倾斜，字体颜色：文字 1
带格式的：默认段落字体，字体颜色：文字 1
带格式的：默认段落字体，字体颜色：文字 1
带格式的：默认段落字体，字体颜色：文字 1，非上标/ 下标
带格式的：默认段落字体，字体颜色：文字 1
带格式的：默认段落字体，字体颜色：文字 1，非上标/ 下标
带格式的：默认段落字体，字体颜色：文字 1
带格式的：下标

The average γ value was consistent with the results derived by the same method in a rural site in Germany (Phillips et al., 2016) but was higher than that found in previous studies in the UK and North America that used different derivation methods; these methods included the steady state lifetime method (Morgan et al., 2015; Brown et al., 2006, 2009), the iterated box model (Wagner et al., 2013) and direct measurement based on an aerosol flow reactor (Bertram et al., 2009; Riedel et al., 2012). The steady state lifetime method is very sensitive to NO_2 concentration, and since the NO_2 measurement suffered with ambient NOy interference, we did not apply the steady state lifetime method in this study (Brown et al., 2003). Nonetheless, the derived γ in Beijing showed good agreement with the recent results derived by the steady state method in Jinan and Mt. Tai (X. F. Wang ~~X~~ et al., 2017; Z. Wang et al., 2017). The consistency eliminates the discrepancy possibly brought by the differences of analysis methods. Therefore, we suggest that fast N_2O_5 uptake was a ubiquitous feature that existed in the NCP. In this study, sulfate is the dominant component of $PM_{1.0}$, accounting for more than 30% of its mass concentration, which may be the reason of elevated N_2O_5 uptake coefficient presented in Beijing, like the result in high sulfate air mass over Ohio and western Pennsylvania (Brown et al., 2006). Previous studies have shown that the N_2O_5 uptake coefficient strongly depends on the liquid water content, the pNO_3^- and organic mass~~; liquid~~. Liquid water content promotes N_2O_5 uptake, whereas pNO_3^- and organic mass inhibit N_2O_5 uptake (e.g., Thornton et al., 2003, Wahner et al., 1998; ~~McNeill et al., 2006~~Bertram and Thornton, 2009). Because of the limited data set of N_2O_5 uptake coefficients in this campaign, the trends of the determined N_2O_5 uptake coefficients with the parameters mentioned above were not convincing, and more valid data is needed for further studies of the N_2O_5 uptake mechanism. With respect to *f*, the values are comparable with that observed in Germany (Phillips et al., 2016) and are similar with that estimated in the power plant plume in Mt. Tai with high chloride content (Z. Wang et al., 2017).

4.2 N_2O_5 lifetime and reactivity

The lifetime of N_2O_5 was estimated by the steady state method, assuming that the production and loss of N_2O_5 was in balance after a period following sunset. Eq. ~~2~~5 for the steady state approximation has been frequently applied in analyzing the fate of N_2O_5 (Platt et al., 1980; Allan et al., 1999; Brown et al., 2003).

$$\tau_{ss}(N_2O_5) = \frac{1}{L_{ss}(N_2O_5)} = \frac{[N_2O_5]}{k_{NO2+O3}[NO_2][O_3]} \qquad \text{(Eq. ~~2~~5)}$$

~~In Eq. 2~~Here $\tau_{ss}(N_2O_5)$ denotes the steady state lifetime of N_2O_5 and $L_{ss}(N_2O_5)$ denotes the loss term of N_2O_5 corresponding to the steady state lifetime. A numerical model was used to check the validity of the steady state approximation (Brown et al., 2003); details are given in Figure ~~S2~~S4. The results show that the steady state can generally be achieved within 30 minutes. In this study, the steady state lifetime was only calculated from 20:00 to the next day 04:00. The time periods with NO concentration larger than 0.~~1~~06 ppbv (instrument LOD) were excluded because the steady state is easily disturbed. The overall N_2O_5 ~~reactivity~~loss rate ($k(N_2O_5)$) can be calculated by accumulating each individual loss term in Eq. ~~3~~6, including the N_2O_5 heterogeneous hydrolysis and the reaction of NO_3 with VOCs.

带格式的：字体颜色：文字 1
带格式的：默认段落字体，字体颜色：文字 1
带格式的：字体颜色：文字 1
带格式的：字体颜色：文字 1
带格式的：字体颜色：文字 1

$$k(N_2O_5) = \frac{\sum k_{NO3+VOCs_i}\cdot[VOCs_i]}{k_{eq}\cdot[NO_2]} + \frac{C\cdot S_a\cdot\gamma}{4} \quad \text{(Eq. 6)}$$

The NO_3 heterogeneous uptake and the loss of N_2O_5 via gas-phase reactions were assumed to be negligible (Brown and Stutz, 2012). ~~k_t~~$k_{NO3+VOCs_i}$ ~~represents~~denotes the reaction rate constants of the reaction of NO_3+$VOCs_i$. Isoprene and monoterpene were used in ~~the~~this calculation.

The N_2O_5 loss rate coefficient by heterogeneous hydrolysis was calculated by using an average γ of 0.034.

$$k(N_2O_5) = \frac{\sum k_t[VOCs_t]}{k_{eq}\cdot[NO_2]} + \frac{C\cdot S_a\cdot\gamma}{4} \quad \text{(Eq. 3)}$$

The time series of the steady state lifetime of N_2O_5 is shown in Figure ~~S3~~S5. The N_2O_5 steady state lifetime ranged from <5 s to ~~1140~~1260 s, with an average of ~~310~~270 ± 240 s, and large variability was shown during the campaign. The N_2O_5 lifetimes during the BAM period were higher than those during the UAM period, which is predictable since the clean air mass has lower N_2O_5 reactivity because of much lower aerosol loading. Two extremely short N_2O_5 lifetime cases were captured on the nights of May 30 and June 3, with peak values below 200 s throughout those nights. Figure ~~7~~6 shows that the N_2O_5 lifetime had a very clear negative dependence of the ambient aerosol surface area when larger than 300 $\mu m^2\ cm^{-3}$, which indicates that the N_2O_5 heterogeneous uptake plays an important role in the regulation of N_2O_5 lifetime. The study conducted in the residual layer of Hong Kong showed a similar tendency despite the overall N_2O_5 lifetime being shorter at this site (Brown et al., 2016). Additionally, a negative dependence of N_2O_5 lifetime on RH was reported in Hong Kong but was not observed in this study (Figure ~~S4).~~S6).

Figure ~~8~~7 shows the time series of the overall N2O5 loss rate constant as well as the N_2O_5 steady state ~~N_2O_5~~ loss rate constant. The overall N2O5 loss rate constant was calculated from the individual terms ~~in (~~Eq.3 ~~was reasonably comparable with ~~). The uncertainties of the N_2O_5 steady state ~~N_2O_5~~ loss rate~~, except for~~ constant and the overall k(N_2O_5) are estimated to be 67% and 95%, respectively (Eq. 7 and Eq. 8). The largest error sources were from the corrected NO_2 measurements so that it is really important to have accurate NO_2 measurement instrument involved in the future campaigns.

$$\frac{\Delta Lss(N_2O_5)}{Lss(N_2O_5)} = \sqrt{(\frac{\Delta[N_2O_5]}{[N_2O_5]})^2 + (\frac{\Delta[NO_2]}{[NO_2]})^2 + (\frac{\Delta[O_3]}{[O_3]})^2 + (\frac{\Delta K_{eq}}{K_{eq}})^2} \quad \text{(Eq. 7)}$$

$$\frac{\Delta k(N_2O_5)}{k(N_2O_5)} = \sqrt{(\frac{\Delta[N_2O_5]}{[N_2O_5]})^2 + (\frac{\Delta[S_a]}{[S_a]})^2 + (\frac{\Delta[\gamma]}{[\gamma]})^2 + (\frac{\Delta[NO_2]}{[NO_2]})^2 + (\frac{\Delta[O_3]}{[O_3]})^2 + (\frac{\Delta[VOC_s]}{[VOC_s]})^2 + (\frac{\Delta K_{eq}}{K_{eq}})^2} \quad \text{(Eq. 8)}$$

On the night of 29 May, the steady state loss rate constant was much lower than the overall k(N_2O_5); on the nights of 28, ~~30~~ May and 3 June, ~~on which~~ the Lss(N2O5) calculated by the steady state method were much higher than the overall k(N2O5~~).~~), but these discrepancies were in the range of the uncertainties. Except the case happened on the night of 30 May, when the steady state loss rate constant was about ten times higher than the overall loss rate constant, and the reason was not well understood according to the available parameters that we have detected. In general, the overall N_2O_5 loss rate constant and the steady state N_2O_5 loss rate constant were comparable taking into considerations of

带格式的: 默认段落字体，字体颜色：文字 1
带格式的: 默认段落字体，字体颜色：文字 1
带格式的: 默认段落字体，字体颜色：文字 1，非上标/ 下标
带格式的: 默认段落字体，字体颜色：文字 1
带格式的: 默认段落字体，字体颜色：文字 1，非上标/ 下标
带格式的: 默认段落字体，字体颜色：文字 1
带格式的: 默认段落字体，字体颜色：文字 1
带格式的: 默认段落字体，字体颜色：文字 1
带格式的: 默认段落字体，字体颜色：文字 1
带格式的: 默认段落字体，字体颜色：文字 1，非上标/ 下标
带格式的: 默认段落字体，字体颜色：文字 1
带格式的: 默认段落字体，字体颜色：文字 1，非上标/ 下标
带格式的: 默认段落字体，字体颜色：文字 1
带格式的: 默认段落字体，字体颜色：文字 1
带格式的: 默认段落字体，字体颜色：文字 1
带格式的: 默认段落字体，字体颜色：文字 1
带格式的: 默认段落字体，字体颜色：文字 1
带格式的: 缩进：首行缩进： 0 字符
带格式的: 默认段落字体，字体颜色：文字 1
带格式的: 默认段落字体，字体颜色：文字 1
带格式的: 默认段落字体，字体颜色：文字 1
带格式的: 默认段落字体，字体：非倾斜，字体颜色：文字 1
带格式的: 默认段落字体，字体颜色：文字 1，非上标/ 下标
带格式的: 默认段落字体，字体颜色：文字 1
带格式的: 默认段落字体，字体颜色：文字 1，非上标/ 下标
带格式的: 默认段落字体，字体颜色：文字 1
带格式的: 默认段落字体，字体颜色：文字 1，非上标/ 下标
带格式的: 默认段落字体，字体颜色：文字 1
带格式的: 默认段落字体，字体颜色：文字 1，非上标/ 下标

the uncertainties. The average N_2O_5 loss rate constant contributed by the N_2O_5 heterogeneous hydrolysis was 8.1×10^{-4} s^{-1}. The average NO_3 loss rate constant by the reaction of NO_3 with VOCs was 0.015 ± 0.007 s^{-1}, which is comparable with the previous results in suburban Beijing in 2006 (H. C. Wang et al., 2017c), in which the contribution to the N_2O_5 reactivity was 1.63×10^{-3} s^{-1}. Compared with N_2O_5 loss via direct heterogeneous hydrolysis, the indirect loss via NO_3+VOCs was dominant, accounting for approximately 67%. Because only a subset of the suite of organic species at the site was measured, the calculated loss rate constant via NO_3+VOCs represents a lower limit. Therefore, the N_2O_5 loss via NO_3+VOCs may occupy a larger proportion. The overall loss rate constant from NO_3+VOCs and N_2O_5 uptake was 2.44×10^{-3} s^{-1}, which was reasonably lower than the steady state N_2O_5 loss rate constant of 3.61×10^{-3} s^{-1}; the gap may be explained by the unmeasured reactive VOCs or the unaccounted NO that was near the instrumental limit of detection.

4.3 ~~Nocturnal~~ NO3-induced nocturnal oxidation of VOCs

Recent studies have suggested that the fate of BVOCs after sunset is dominated by ~~NO_x~~NO_x or O_3, with variation of the ratio of ~~NO_x~~NO_x to BVOCs and that the nighttime oxidation is located in the transition region between ~~NO_x~~NO_x-domination and O_3-domination in the United States (Edwards et al., 2017). During this campaign, the nocturnal average concentrations of isoprene and monoterpene were 156 ± 88 pptv and 86 ± 42 pptv, respectively. We used isoprene and monoterpene to represent a lower limit mixing ratio of total BVOCs; the average ratio of ~~NO_x/BVOC~~NO_x/BVOCs was larger than 10 and exhibited small variation during the BAM and UAM periods. The value was much higher than the critical value (~~NO_x~~NO_x /BVOC = 0.5) of the transition regime proposed by Edwards et al. (2017), which suggests that the oxidation of BVOCs in Beijing was NO_x-dominated and the nighttime fate of BVOCs was controlled by NO_3. Since the ONs formation via BVOC oxidation was mainly attributed to the NO_3 oxidation with high yield, we suggest that the ONs production capacity was maximized in the high NO_x/BVOCs region.

The pseudo first order loss rate of VOCs initialed by oxidants, $k(VOCs_i)$, is defined as VOCs reactivity and expressed as Eq. ~~4~~9. Here, we only consider the reaction of VOCs with O_3 and NO_3. ~~$k_{VOCs_i+NO_3}$ and $k_{VOCs_i+O_3}$ are~~$k_{O_3+VOCs_i}$ denotes the reaction rate constants of $VOCs_i$ with ~~NO_3 and O_3, respectively~~.

$$k(VOCs_i) = \sout{k_{VOCs_i+NO_3}} = k_{NO_3+VOCs_i}\cdot[NO_3] \sout{+ k_{VOCs_i+O_3}} + k_{O_3+VOCs_i}\cdot[O_3] \quad \text{(Eq. 4}\sout{8}\text{9)}$$

During this campaign, VOCs reactivity could be determined with the measured O_3 and calculated NO_3. Figure ~~9~~8 depicts four kinds of VOCs reactivity distribution during nighttime, including the isoprene (ISO), monoterpene (~~here represented by α-pinene, API~~MNT), the double bond at the end or terminal position of the molecule (OLT) and alkenes with the double bond elsewhere in the molecule (OLI). The reaction rates were cited from the regional atmospheric chemistry mechanism version 2 (RACM2, Goliff et al., (2013)). Previous measurement indicated the main detectable monoterpenes were α-pinene and β-pinene in summer Beijing (personal communication with Ying Liu). Here we assumed *α*-pinene and *β*-pinene occupies half and half in the monoterpene. The average value of the rate coefficient of *α*-pinene and *β*-pinene with NO_3 was used as the rate coefficient of monoterpene with NO_3 (Atkinson and Arey, 2003). The uncertainty of the monoterpene + NO_3 rate coefficient in these

带格式的: 默认段落字体, 字体颜色: 文字 1
带格式的: 字体: Times New Roman
带格式的: 默认段落字体, 字体: 非加粗, 字体颜色: 文字 1
带格式的: 默认段落字体, 字体: 非加粗, 字体颜色: 文字 1, 非上标/ 下标
带格式的: 默认段落字体, 字体: 非加粗, 字体颜色: 文字 1, 非上标/ 下标
带格式的: 默认段落字体, 字体: 非加粗, 字体颜色: 文字 1
带格式的: 默认段落字体, 字体颜色: 文字 1
带格式的: 默认段落字体, 字体: 倾斜, 字体颜色: 文字 1, 下标
带格式的: 默认段落字体, 字体颜色: 文字 1
带格式的: 默认段落字体, 字体: 倾斜, 字体颜色: 文字 1, 下标
带格式的: 字体: 倾斜

air masses is thus estimated to be 50%. The uncertainty of calculated NO_3 is 67%. The uncertainty of the reaction rate efficiency of NO_3+monoterpene (50%) was calculated by the Gaussian propagation method and the overall uncertainty of monoterpene reactivity was calculated to be 85%, the uncertainties of other VOCs was calculated to be 75% by assuming the uncertainties of rate efficiencies were 30%. The VOCs reactivity were dominated by NO_3 oxidation and contributed up to 90% in total; less than 10% VOCs were oxidized by O_3 during the nighttime. ~~The~~Even the NO_3 concentration in the lower range, NO_3 still responsible for more than 70% nocturnal BVOCs oxidation, the results further confirmed that the oxidation of BVOCs is controlled by NO_3 rather than O_3~~.~~ in summer Beijing.

For calculating nocturnal ONs production from NO_3 oxidation of isoprene and monoterpene, as well as ~~the same period~~ inorganic nitrate production via N_2O_5 heterogeneous uptake over the same period, the $ClNO_2$ yield was set to the determined average value of 0.55. The organic nitrate yield of the reaction of NO_3 with isoprene was set to 0.7, from Rollins et al. (2009). The yield from the reaction of NO_3 with monoterpene was represented by NO_3 +α-pinene and was set to 0.15, following Spittler et al. (2006). Although the yield from the NO_3 oxidation of isoprene is much higher than that of monoterpene, the total ONs production was dominated by the oxidation of NO_3 with monoterpene because the reaction of NO_3 with monoterpene is much faster than that with isoprene. Because of the lack of measurement of alkenes and other VOCs that can react with NO_3 and form ONs, the calculated nighttime ONs production rate analyzed here served as lower limit estimations. Figure ~~10~~9 depicts the mean diurnal profiles of the nocturnal formation rates of inorganic nitrates and ONs. The average production rate of ONs was up to 0.~~11~~10 ± 0.~~09~~07 ppbv h^{-1}, which was ~~much~~ higher than that predicted in a suburban site in Beijing in 2006, with an average value of 0.06 ppbv h^{-1} (H.C. Wang et al., 2017b). In the high ~~NO_x~~NO_x/BVOCs air masses, the inorganic nitrate formation was proposed to increase with the increase of sunset ~~NO_x~~NO_x/BVOCs (Edwards et al., 2017). The formation rate of inorganic nitrate via N_2O_5 uptake was significant, with an average of 0.43 ± 0.12 ppbv h^{-1}, and was much larger than the organic nitrate formation. ~~The~~ NO_x was mainly removed as the inorganic nitrate format by nocturnal NO_3-N_2O_5 chemistry in Beijing. Overall, the NO_3-N_2O_5 chemistry led to significant ~~NO_x~~NO_x removal, with 0.54 ppbv h^{-1} accounted for by the organic and inorganic nitrates, and the integral ~~NO_x~~NO_x removal was approximately 5 ppbv per night. Since ONs are important precursors of the secondary organic aerosols (SOA), the NO_3 oxidation was very important from the perspective of organic aerosol formation and regional particulate matter (e.g., Ng et al., 2008).

5. Conclusion

We reported an intensive field study of NO_3-N_2O_5 chemistry at a downwind suburban site in Beijing during the summer of 2016. High levels of $ClNO_2$ and N_2O_5 were observed, with maxima of 2.9 ppbv and 937 pptv (1-min), respectively. The N_2O_5 uptake coefficient was estimated to be in the range of 0.010-0.055, with an average value of 0.034 ± 0.018, and the corresponding $ClNO_2$ yield was derived to be in the range of 0.5-1.0, with an average value of 0.73 ± 0.25. The elevated $ClNO_2$ levels and $ClNO_2$/N_2O_5 ratios are comparable with those in chloride-rich regions in the NCP. The results highlight fast N_2O_5 heterogeneous hydrolysis and efficient $ClNO_2$ formation in the outflow of urban Beijing. Thus, its role in O_3 pollution in summer could be more important than in other regions.

带格式的: 字体: 倾斜, 字体颜色: 文字 1

带格式的: 默认段落字体, 字体颜色: 文字 1

带格式的: 默认段落字体, 字体: 倾斜, 字体颜色: 文字 1, 下标

Since the NO_3-N_2O_5 chemical equilibrium favors NO_3 in summer with high temperature and high NO_x, the elevated NO_3 dominated the nocturnal degradation of BVOCs and could lead to efficient ONs formation. Because the air masses in Beijing featured high ~~NO_x~~NO_x/BVOCs ratios (>10), our results suggest that the nocturnal NO_3 oxidation of BVOCs was NO_x-dominated. Because of the extremely high NO_x emissions, the formation of ONs may not be sensitive to the reduction of NO_x but rather to the change of unsaturated VOCs (e.g., BVOCs), which is similar to the daytime photochemical O_3 pollution (e.g., Lu et al., 2010) diagnosed for this area; this suggests that the control of the unsaturated VOCs would moderate the O_3 pollution and ONs particulate matter in parallel. Moreover, the reduction of NO_x would also be helpful to reduce the pNO_3^- formation via N_2O_5 heterogeneous hydrolysis under such high NO_x/BVOCs ratios (Edwards et al., 2017).

Acknowledgements. This work was supported by the National Natural Science Foundation of China (Grants No. 91544225, 41375124, 21522701, 41421064, 91744204), the National Science and Technology Support Program of China (No. 2014BAC21B01), the Strategic Priority Research Program of the Chinese Academy of Sciences (Grants No. XDB05010500), and the program on ~~‘~~“Photochemical smog in China” financed by the Swedish Research Council (639-2013-6917). The authors gratefully acknowledge the Peking University and Gethenburg University science team for their technical support and discussions during the Changping campaign.

Reference

Allan, B. J., Carslaw, N., Coe, H., Burgess, R. A., and Plane, J. M. C.: Observations of the nitrate radical in the marine boundary layer, J Atmos Chem, 33, 129-154, Doi10.1023/A:1005917203307, 1999.

Bannan, T. J., Booth, A. M., Bacak, A., Muller, J. B. A., Leather, K. E., Le Breton, M., Jones, B., Young, D., Coe, H., Allan, J., Visser, S., Slowik, J. G., Furger, M., Prevot, A. S. H., Lee, J., Dunmore, R. E., Hopkins, J. R., Hamilton, J. F., Lewis, A. C., Whalley, L. K., Sharp, T., Stone, D., Heard, D. E., Fleming, Z. L., Leigh, R., Shallcross, D. E., and Percival, C. J.: The first UK measurements of nitryl chloride using a chemical ionization mass spectrometer in central London in the summer of 2012, and an investigation of the role of Cl atom oxidation, J Geophys Res-Atmos, 120, 5638-5657, 10.1002/2014jd022629, 2015.

Benton, A. K., Langridge, J. M., Ball, S. M., Bloss, W. J., Dall'Osto, M., Nemitz, E., Harrison, R. M., and Jones, R. L.: Night-time chemistry above London: measurements of NO_3 and N_2O_5 from the BT Tower, Atmos Chem Phys, 10, 9781-9795, 10.5194/acp-10-9781-2010, 2010.

Bertram, T. H., and Thornton, J. A.: Toward a general parameterization of N_2O_5 reactivity on aqueous particles: the competing effects of particle liquid water, nitrate and chloride, Atmos Chem Phys, 9, 8351-8363, 2009.

Bertram, T. H., Thornton, J. A., Riedel, T. P., Middlebrook, A. M., Bahreini, R., Bates, T. S., Quinn, P. K., and Coffman, D. J.: Direct observations of N_2O_5 reactivity on ambient aerosol particles, Geophys Res Lett, 36, Artn L19803.10.1029/2009gl040248, 2009.

带格式的：默认段落字体，字体颜色：文字 1
带格式的：默认段落字体，字体：倾斜，字体颜色：文字 1，下标
带格式的：默认段落字体，字体颜色：文字 1
带格式的：默认段落字体，字体：倾斜，字体颜色：文字 1，下标
带格式的：默认段落字体，字体颜色：文字 1
带格式的：默认段落字体，字体：倾斜，字体颜色：文字 1，下标
带格式的：默认段落字体，字体颜色：文字 1
带格式的：默认段落字体，字体：倾斜，字体颜色：文字 1，下标
带格式的：默认段落字体，字体颜色：文字 1
带格式的：默认段落字体，字体：倾斜，字体颜色：文字 1，下标
带格式的：默认段落字体，字体颜色：文字 1
带格式的：默认段落字体，字体：倾斜，字体颜色：文字 1，下标
带格式的：fontstyle01
带格式的：默认段落字体，字体：AdvTTf331adb4.B，11 磅，字体颜色：文字 1
带格式的：默认段落字体，字体颜色：文字 1

Bohn, B., Corlett, G. K., Gillmann, M., Sanghavi, S., Stange, G., Tensing, E., Vrekoussis, M., Bloss, W. J., Clapp, L. J., Kortner,M., Dorn, H.-P., Monks, P. S., Platt, U., Plass-Dülmer, C., Mihalopoulos, N., Heard, D. E., Clemitshaw, K. C., Meixner, F. X.,Prevot, A. S. H., and Schmitt, R.: Photolysis frequency measurement techniques: results of a comparison within the ACCENTproject, Atmos. Chem. Phys., 8, 5373–5391, doi:10.5194/acp-8-5373-2008, 2008.

Behnke, W., George, C., Scheer, V., and Zetzsch, C.: Production and decay of ClNO2, from the reaction of gaseous N2O5 with NaCl solution: Bulk and aerosol experiments, J Geophys Res-Atmos, 102, 3795-3804, Doi 10.1029/96jd03057, 1997.

Boyd, C. M., Nah, T., Xu, L., Berkemeier, T., and Ng, N. L.: Secondary Organic Aerosol (SOA) from Nitrate Radical Oxidation of Monoterpenes: Effects of Temperature, Dilution, and Humidity on Aerosol Formation, Mixing, and Evaporation, Environ Sci Technol, 51, 7831-7841, 2017.

Brown, S. S., Stark, H., and Ravishankara, A. R.: Applicability of the steady state approximation to the interpretation of atmospheric observations of NO_3 and N_2O_5, J Geophys Res-Atmos, 108, Artn 4539.Doi 10.1029/2003jd003407, 2003.

Brown, S. S., Ryerson, T. B., Wollny, A. G., Brock, C. A., Peltier, R., Sullivan, A. P., Weber, R. J., Dube, W. P., Trainer, M., Meagher, J. F., Fehsenfeld, F. C., and Ravishankara, A. R.: Variability in nocturnal nitrogen oxide processing and its role in regional air quality, Science, 311, 67-70, DOI 10.1126/science.1120120, 2006.

Brown, S. S., Dube, W. P., Fuchs, H., Ryerson, T. B., Wollny, A. G., Brock, C. A., Bahreini, R., Middlebrook, A. M., Neuman, J. A., Atlas, E., Roberts, J. M., Osthoff, H. D., Trainer, M., Fehsenfeld, F. C., and Ravishankara, A. R.: Reactive uptake coefficients for N_2O_5 determined from aircraft measurements during the Second Texas Air Quality Study: Comparison to current model parameterizations, J Geophys Res-Atmos, 114, Artn D00f10. Doi 10.1029/2008jd011679, 2009.

Brown, S. S., and Stutz, J.: Nighttime radical observations and chemistry, Chem Soc Rev, 41, 6405-6447, Doi 10.1039/C2cs35181a, 2012.

Brown, S. S., Dube, W. P., Tham, Y. J., Zha, Q. Z., Xue, L. K., Poon, S., Wang, Z., Blake, D. R., Tsui, W., Parrish, D. D., and Wang, T.: Nighttime chemistry at a high altitude site above Hong Kong, J Geophys Res-Atmos, 121, 2457-2475, 10.1002/2015jd024566, 2016.

Chang, W. L., Bhave, P. V., Brown, S. S., Riemer, N., Stutz, J., and Dabdub, D.: Heterogeneous Atmospheric Chemistry, Ambient Measurements, and Model Calculations of N_2O_5: A Review, Aerosol Sci Tech, 45, 665-695, 2011.

DeCarlo, P. F., Kimmel, J., Trimborn, A., Northway, M., Jayne, J. T., Aiken, A., Gonin, M., Fuhrer, K., Horvath, T., Docherty, K., Worsnop, D. R., and Jimenez, J. L.: Field-deployable, high-resolution, time-of-flight Aerosol Mass Spectrometer, Anal. Chem., 78, 8281-8289, 2006.

de Gouw, J. and Warneke, C.: Measurements of volatile organic compounds in the earth's atmosphere using proton-transferreaction mass spectrometry, Mass Spectrom. Rev., 26, 223-257, 2007.

~~Dong, H. B., Zeng, L. M., Hu, M., Wu, Y. S., Zhang, Y. H., Slanina, J., Zheng, M., Wang, Z. F., and Jansen, R.: Technical Note: The application of an improved gas and aerosol collector for ambient air pollutants in China, Atmos Chem Phys, 12, 10519-10533, 2012.~~

Draxler, R. R., and G. D. Rolph: HYSPLIT (HYbrid Single-Particle Lagrangian Integrated Tracker) Model access via NOAA ARL Ready Website [Available at http://www.arl.noaa.gov/ready/hysplit4.html, NOAA Air Resources Laboratory, Silver Spring, MD]. 2003.

Edwards, P. M., Aikin, K. C., Dube, W. P., Fry, J. L., Gilman, J. B., de Gouw, J. A., Graus, M. G., Hanisco, T. F., Holloway, J., Huber, G., Kaiser, J., Keutsch, F. N., Lerner, B. M., Neuman, J. A., Parrish, D. D., Peischl, J., Pollack, I. B., Ravishankara, A. R., Roberts, J. M., Ryerson, T. B., Trainer, M., Veres, P. R., Wolfe, G. M., Warneke, C., and Brown, S. S.: Transition from high- to low-NOx control of night-time oxidation in the southeastern US, Nat Geosci, 10, 490-+, 10.1038/Ngeo2976, 2017.

Faxon, C. B., Bean, J. K., and Ruiz, L. H.: Inland Concentrations of Cl_2 and $ClNO_2$ in Southeast Texas suggest chlorine chemistry significantly contributes to atmospheric reactivity, Atmosphere, 6, 1487–1506, 2015.

~~Finlaysonpitts~~Finlayson-Pitts, B. J., Ezell, M. J., and Pitts, J. N.: Formation of Chemically Active Chlorine Compounds by Reactions of Atmospheric Nacl Particles with Gaseous N_2O_5 and $ClONO_2$, Nature, 337, 241-244, DOI 10.1038/337241a0, 1989.

Fry, J. L., Kiendler-Scharr, A., Rollins, A. W., Wooldridge, P. J., Brown, S. S., Fuchs, H., Dube, W., Mensah, A., dal Maso, M., Tillmann, R., Dorn, H. P., Brauers, T., and Cohen, R. C.: Organic nitrate and secondary organic aerosol yield from NO_3 oxidation of beta-pinene evaluated using a gas-phase kinetics/aerosol partitioning model, Atmos Chem Phys, 9, 1431-1449, 2009.

Gaston, C. J., Thornton, J. A., and Ng, N. L.: Reactive uptake of N_2O_5 to internally mixed inorganic and organic particles: the role of organic carbon oxidation state and inferred organic phase separations, Atmos Chem Phys, 14, 5693-5707, 10.5194/acp-14-5693-2014, 2014.

Geyer, A., Alicke, B., Konrad, S., Schmitz, T., Stutz, J., and Platt, U.: Chemistry and oxidation capacity of the nitrate radical in the continental boundary layer near Berlin, J Geophys Res-Atmos, 106, 8013-8025, Doi 10.1029/2000jd900681, 2001.

Goliff, W. S., Stockwell, W. R., and Lawson, C. V.: The regional atmospheric chemistry mechanism, version 2, Atmos Environ, 68, 174-185, 2013.

Grzinic, G., Bartels-Rausch, T., Berkemeier, T., Turler, A., and Ammann, M.: Viscosity controls humidity dependence of N_2O_5 uptake to citric acid aerosol, Atmos Chem Phys, 15, 13615-13625, 2015.

Hallquist, M., Stewart, D. J., Stephenson, S. K., and Cox, R. A.: Hydrolysis of N_2O_5 on sub-micron sulfate aerosols, Phys Chem Chem Phys, 5, 3453-3463, Doi 10.1039/B301827j, 2003.

Hallquist, M., Munthe, J., Hu, M., Wang, T., Chan, C. K., Gao, J., Boman, J., Guo, S., Hallquist, A. M., Mellqvist, J., Moldanova, J., Pathak, R. K., Pettersson, J. B. C., Pleijel, H., Simpson, D., and Thynell, M.: Photochemical smog in China: scientific challenges and implications for air-quality policies, Natl Sci Rev, 3, 401-403, 10.1093/nsr/nww080, 2016.

Kiendler-Scharr, A., Mensah, A. A., Friese, E., Topping, D., Nemitz, E., Prevot, A. S. H., Aijala, M., Allan, J., Canonaco, F., Canagaratna, M., Carbone, S., Crippa, M., Dall Osto, M., Day, D. A., De Carlo, P., Di Marco, C. F., Elbern, H., Eriksson, A., Freney, E., Hao, L., Herrmann, H., Hildebrandt, L., Hillamo, R., Jimenez, J. L., Laaksonen, A., McFiggans, G., Mohr, C., O'Dowd, C., Otjes, R., Ovadnevaite, J., Pandis, S. N., Poulain, L., Schlag, P., Sellegri, K., Swietlicki, E., Tiitta, P., Vermeulen, A., Wahner, A., Worsnop, D., and Wu, H. C.: Ubiquity of organic nitrates from nighttime chemistry in the European submicron aerosol, Geophys Res Lett, 43, 7735-7744, 2016.

Le Breton, M., Bacak, A., Muller, J. B. A., Bannan, T. J., Kennedy, O., Ouyang, B., Xiao, P., Bauguitte, S. J. B., Shallcross, D. E., Jones, R. L., Daniels, M. J. S., Ball, S. M., and Percival, C. J.: The first airborne comparison of N_2O_5 measurements over the UK using a CIMS and BBCEAS during the RONOCO campaign, Anal Methods-Uk, 6, 9731-9743, 10.1039/c4ay02273d, 2014.

Le Breton, M., Hallquist, Å. M., Pathak, R. K., Simpson, D., Wang, Y., Johansson, J., Zheng, J., Yang, Y., Shang, D., Wang, H., Liu, Q., Chan, C., Wang, T., Bannan, T. J., Priestley, M., Percival, C. J., Shallcross, D. E., Lu, K., Guo, S., Hu, M., and Hallquist, M.: Chlorine oxidation of VOCs at a semi-rural site in Beijing: Significant chlorine liberation from $ClNO_2$ and subsequent gas and particle phase Cl-VOC production, Atmos. Chem. Phys. Discuss., 2018, 1-25, 2018.

Li, S. W., Liu, W. Q., Xie, P. H., Qin, M., and Yang, Y. J.: Observation of Nitrate Radical in the Nocturnal Boundary Layer During a Summer Field Campaign in Pearl River Delta, China, Terr Atmos Ocean Sci, 23, 39-48, Doi 10.3319/Tao.2011.07.26.01(a), 2012.

Li, Q. Y., Zhang, L., Wang, T., Tham, Y. J., Ahmadov, R., Xue, L. K., Zhang, Q., and Zheng, J. Y.: Impacts of heterogeneous uptake of dinitrogen pentoxide and chlorine activation on ozone and reactive nitrogen partitioning: improvement and application of the WRF-Chem model in southern China, Atmos Chem Phys, 16, 14875-14890, 10.5194/acp-16-14875-2016, 2016.

Liu, X. G., Gu, J. W., Li, Y. P., Cheng, Y. F., Qu, Y., Han, T. T., Wang, J. L., Tian, H. Z., Chen, J., and Zhang, Y. H.: Increase of aerosol scattering by hygroscopic growth: Observation, modeling, and implications on visibility, Atmos Res, 132, 91-101, 10.1016/j.atmosres.2013.04.007, 2013.

Liu, M. X., Song, Y., Zhou, T., Xu, Z. Y., Yan, C. Q., Zheng, M., Wu, Z. J., Hu, M., Wu, Y. S., and Zhu, T.: Fine particle pH during severe haze episodes in northern China, Geophys Res Lett, 44, 5213-5221, 10.1002/2017gl073210, 2017.

Lopez-Hilfiker, F. D., Mohr, C., Ehn, M., Rubach, F., Kleist, E., Wildt, J., Mentel, T. F., Lutz, A., Hallquist, M., Worsnop, D., and Thornton, J. A.: A novel method for online analysis of gas and particle composition: description and evaluation of a Filter Inlet for Gases and AEROsols (FIGAERO), Atmos Meas Tech, 7, 983-1001, 10.5194/amt-7-983-2014, 2014.

Lu, K. D., Zhang, Y. H., Su, H., Brauers, T., Chou, C. C., Hofzumahaus, A., Liu, S. C., Kita, K., Kondo, Y., Shao, M., Wahner, A., Wang, J. L., Wang, X. S., and Zhu, T.: Oxidant (O_3 + NO_2) production processes and formation regimes in Beijing, J Geophys Res-Atmos, 115, 2010.

McLaren, R., Wojtal, P., Majonis, D., McCourt, J., Halla, J. D., and Brook, J.: NO_3 radical measurements in a polluted marine environment: links to ozone formation, Atmos Chem Phys, 10, 4187-4206, 10.5194/acp-10-4187-2010, 2010.

~~McNeill, V. F., Patterson, J., Wolfe, G. M., and Thornton, J. A.: The effect of varying levels of surfactant on the reactive uptake of N_2O_5 to aqueous aerosol, Atmos Chem Phys, 6, 1635-1644, 2006.~~

Mentel, T. F., Sohn, M., and Wahner, A.: Nitrate effect in the heterogeneous hydrolysis of dinitrogen pentoxide on aqueous aerosols, Phys Chem Chem Phys, 1, 5451-5457, Doi 10.1039/A905338g, 1999.

Mielke, L. H., Furgeson, A., and Osthoff, H. D.: Observation of $ClNO_2$ in a Mid-Continental Urban Environment, Environ Sci Technol, 45, 8889-8896, 10.1021/es201955u, 2011.

Mielke, L. H., Stutz, J., Tsai, C., Hurlock, S. C., Roberts, J. M., Veres, P. R., Froyd, K. D., Hayes, P. L., Cubison, M. J., Jimenez, J. L., Washenfelder, R. A., Young, C. J., Gilman, J. B., de Gouw, J. A., Flynn, J. H., Grossberg, N., Lefer, B. L., Liu, J., Weber, R. J., and Osthoff, H. D.: Heterogeneous formation of nitryl chloride and its role as a nocturnal NOx reservoir species during CalNex-LA 2010, J Geophys Res-Atmos, 118, 10638-10652, Doi 10.1002/Jgrd.50783, 2013.

Morgan, W. T., Ouyang, B., Allan, J. D., Aruffo, E., Di Carlo, P., Kennedy, O. J., Lowe, D., Flynn, M. J., Rosenberg, P. D., Williams, P. I., Jones, R., McFiggans, G. B., and Coe, H.: Influence of aerosol chemical composition on N_2O_5 uptake: airborne regional measurements in northwestern Europe, Atmos Chem Phys, 15, 973-990, DOI 10.5194/acp-15-973-2015, 2015.

Ng, N. L., Kwan, A. J., Surratt, J. D., Chan, A. W. H., Chhabra, P. S., Sorooshian, A., Pye, H. O. T., Crounse, J. D., Wennberg, P. O., Flagan, R. C., and Seinfeld, J. H.: Secondary organic aerosol (SOA) formation from reaction of isoprene with nitrate radicals (NO3), Atmos Chem Phys, 8, 4117-4140, 2008.

Ng, N. L., Brown, S. S., Archibald, A. T., Atlas, E., Cohen, R. C., Crowley, J. N., Day, D. A., Donahue, N. M., Fry, J. L., Fuchs, H., Griffin, R. J., Guzman, M. I., Herrmann, H., Hodzic, A., Iinuma, Y., Jimenez, J. L., Kiendler-Scharr, A., Lee, B. H., Luecken, D. J., Mao, J. Q., McLaren, R., Mutzel, A., Osthoff, H. D., Ouyang, B., Picquet-Varrault, B., Platt, U., Pye, H. O. T., Rudich, Y., Schwantes, R. H., Shiraiwa, M., Stutz, J., Thornton, J. A., Tilgner, A., Williams, B. J., and Zaveri, R. A.: Nitrate radicals and biogenic volatile organic compounds: oxidation, mechanisms, and organic aerosol, Atmos Chem Phys, 17, 2103-2162, 10.5194/acp-17-2103-2017, 2017.

Osthoff, H. D., Roberts, J. M., Ravishankara, A. R., Williams, E. J., Lerner, B. M., Sommariva, R., Bates, T. S., Coffman, D., Quinn, P. K., Dibb, J. E., Stark, H., Burkholder, J. B., Talukdar, R. K., Meagher, J., Fehsenfeld, F. C., and Brown, S. S.: High levels of nitryl chloride in the polluted subtropical marine boundary layer, Nat Geosci, 1, 324-328, Doi 10.1038/Ngeo177, 2008.

Phillips, G. J., Thieser, J., Tang, M. J., Sobanski, N., Schuster, G., Fachinger, J., Drewnick, F., Borrmann, S., Bingemer, H., Lelieveld, J., and Crowley, J. N.: Estimating N_2O_5 uptake coefficients using ambient measurements of NO_3, N_2O_5, $ClNO_2$ and particle-phase nitrate, Atmos Chem Phys, 16, 13231-13249, 10.5194/acp-16-13231-2016, 2016.

Platt, U., Perner, D., Winer, A. M., Harris, G. W., and Pitts, J. N.: Detection of NO_3 in the Polluted Troposphere by Differential Optical-Absorption, Geophys Res Lett, 7, 89-92, Doi 10.1029/Gl007i001p00089, 1980.

Pye, H. O. T., Chan, A. W. H., Barkley, M. P., and Seinfeld, J. H.: Global modeling of organic aerosol: the importance of reactive nitrogen (NOx and NO_3), Atmos Chem Phys, 10, 11261-11276, 2010.

Riedel, T. P., Bertram, T. H., Ryder, O. S., Liu, S., Day, D. A., Russell, L. M., Gaston, C. J., Prather, K. A., and Thornton, J. A.: Direct N2O5 reactivity measurements at a polluted coastal site, Atmos Chem Phys, 12, 2959-2968, DOI 10.5194/acp-12-2959-2012, 2012.

Riedel, T. P., Wolfe, G. M., Danas, K. T., Gilman, J. B., Kuster, W. C., Bon, D. M., Vlasenko, A., Li, S. M., Williams, E. J., Lerner, B. M., Veres, P. R., Roberts, J. M., Holloway, J. S., Lefer, B., Brown, S. S., and Thornton, J. A.: An MCM modeling study of nitryl chloride ($ClNO_2$) impacts on oxidation, ozone production and nitrogen oxide partitioning in polluted continental outflow, Atmos Chem Phys, 14, 3789-3800, 10.5194/acp-14-3789-2014, 2014.

Riemer, N., Vogel, H., Vogel, B., Anttila, T., Kiendler-Scharr, A., and Mentel, T. F.: Relative importance of organic coatings for the heterogeneous hydrolysis of N2O5 during summer in Europe, J Geophys Res-Atmos, 114, 2009.

Roberts, J. M., Osthoff, H. D., Brown, S. S., Ravishankara, A. R., Coffman, D., Quinn, P., and Bates, T.: Laboratory studies of products of N_2O_5 uptake on Cl^- containing substrates, Geophys Res Lett, 36, Artn L20808. 10.1029/2009gl040448, 2009.

Rollins, A. W., Kiendler-Scharr, A., Fry, J. L., Brauers, T., Brown, S. S., Dorn, H. P., Dube, W. P., Fuchs, H., Mensah, A., Mentel, T. F., Rohrer, F., Tillmann, R., Wegener, R., Wooldridge, P. J., and Cohen, R. C.: Isoprene oxidation by nitrate radical: alkyl nitrate and secondary organic aerosol yields, Atmos Chem Phys, 9, 6685-6703, 2009.

Sarwar, G., Simon, H., Xing, J., and Mathur, R.: Importance of tropospheric $ClNO_2$ chemistry across the Northern Hemisphere, Geophys Res Lett, 41, 4050-4058, 10.1002/2014gl059962, 2014.

Spittler, M., Barnes, I., Bejan, I., Brockmann, K. J., Benter, T., and Wirtz, K.: Reactions of NO_3 radicals with limonene and alpha-pinene: Product and SOA formation, Atmos Environ, 40, S116-S127, 10.1016/j.atmosenv.2005.09.093, 2006.

Stutz, J., Wong, K. W., Lawrence, L., Ziemba, L., Flynn, J. H., Rappengluck, B., and Lefer, B.: Nocturnal NO_3 radical chemistry in Houston, TX, Atmos Environ, 44, 4099-4106, 10.1016/j.atmosenv.2009.03.004, 2010.

Su, X., Tie, X. X., Li, G. H., Cao, J. J., Huang, R. J., Feng, T., Long, X., and Xu, R. G.: Effect of hydrolysis of N_2O_5 on nitrate and ammonium formation in Beijing China: WRF-Chem model simulation, Sci Total Environ, 579, 221-229, 10.1016/j.scitotenv.2016.11.125, 2017.

Tan, Z., Fuchs, H., Lu, K., Hofzumahaus, A., Bohn, B., Broch, S., Dong, H., Gomm, S., Häseler, R., He, L., Holland, F., Li, X., Liu, Y., Lu, S., Rohrer, F., Shao, M., Wang, B., Wang, M., Wu, Y., Zeng, L., Zhang, Y., Wahner, A., and Zhang, Y.: Radical chemistry at a rural site (Wangdu) in the North China Plain: observation and model calculations of OH, HO_2 and RO_2 radicals, Atmos. Chem. Phys., 17, 663-690, 10.5194/acp-17-663-2017, 2017.

Tang, M. J., Schuster, G., and Crowley, J. N.: Heterogeneous reaction of N_2O_5 with illite and Arizona test dust particles, Atmos Chem Phys, 14, 245-254, 2014.

Tang, M. J., Thieser, J., Schuster, G., and Crowley, J. N.: Kinetics and mechanism of the heterogeneous reaction of N_2O_5 with mineral dust particles, Phys Chem Chem Phys, 14, 8551-8561, 2012.

~~Tang, M., Huang, X., Lu, K., Ge, M., Li, Y., Cheng, P., Zhu, T., Ding, A., Zhang, Y., Gligorovski, S., Song, W., Ding, X., Bi, X., and Wang, X.: Heterogeneous reactions of mineral dust aerosol: implications for tropospheric oxidation capacity, Atmos. Chem. Phys., 17, 11727-11777, https://doi.org/10.5194/acp-17-11727-2017, 2017.~~

Tham, Y. J., Wang, Z., Li, Q. Y., Yun, H., Wang, W. H., Wang, X. F., Xue, L. K., Lu, K. D., Ma, N., Bohn, B., Li, X., Kecorius, S., Gross, J., Shao, M., Wiedensohler, A., Zhang, Y. H., and Wang, T.: Significant concentrations of nitryl chloride sustained in the morning: investigations of the causes and impacts on ozone production in a polluted region of northern China, Atmos Chem Phys, 16, 14959-14977, 10.5194/acp-16-14959-2016, 2016.

Thornton, J. A., Braban, C. F., and Abbatt, J. P. D.: N_2O_5 hydrolysis on sub-micron organic aerosols: the effect of relative humidity, particle phase, and particle size, Phys Chem Chem Phys, 5, 4593-4603, Doi 10.1039/B307498f, 2003.

Thornton, J. A., and Abbatt, J. P. D.: N_2O_5 reaction on submicron sea salt aerosol: Kinetics, products, and the effect of surface active organics, J Phys Chem A, 109, 10004-10012, Doi 10.1021/Jp054183t, 2005.

Thornton, J. A., Kercher, J. P., Riedel, T. P., Wagner, N. L., Cozic, J., Holloway, J. S., Dube, W. P., Wolfe, G. M., Quinn, P. K., Middlebrook, A. M., Alexander, B., and Brown, S. S.: A large atomic chlorine source inferred from mid-continental reactive nitrogen chemistry, Nature, 464, 271-274, Doi 10.1038/Nature08905, 2010.

Wagner, N. L., Riedel, T. P., Young, C. J., Bahreini, R., Brock, C. A., Dube, W. P., Kim, S., Middlebrook, A. M., Ozturk, F., Roberts, J. M., Russo, R., Sive, B., Swarthout, R., Thornton, J. A., VandenBoer, T. C., Zhou, Y., and Brown, S. S.: N_2O_5 uptake coefficients and nocturnal NO_2 removal rates determined from ambient wintertime measurements, J Geophys Res-Atmos, 118, 9331-9350, Doi 10.1002/Jgrd.50653, 2013.

Wahner, A., Mentel, T. F., and Sohn, M.: Gas-phase reaction of N_2O_5 with water vapor: Importance of heterogeneous hydrolysis of N_2O_5 and surface desorption of HNO3 in a large teflon chamber, Geophys Res Lett, 25, 2169-2172, Doi 10.1029/98gl51596, 1998.

Wang, S. S., Shi, C. Z., Zhou, B., Zhao, H., Wang, Z. R., Yang, S. N., and Chen, L. M.: Observation of NO_3 radicals over Shanghai, China, Atmos Environ, 70, 401-409, DOI 10.1016/j.atmosenv.2013.01.022, 2013.

Wang, M., Shao, M., Chen, W., Yuan, B., Lu, S., Zhang, Q., Zeng, L., and Wang, Q.: A temporally and spatially resolved validation of emission inventories by measurements of ambient volatile organic compounds in Beijing, China, Atmos Chem Phys, 14, 5871-5891, 10.5194/acp-14-5871-2014, 2014.

Wang, D., Hu, R. Z., Xie, P. H., Liu, J. G., Liu, W. Q., Qin, M., Ling, L. Y., Zeng, Y., Chen, H., Xing, X. B., Zhu, G. L., Wu, J., Duan, J., Lu, X., and Shen, L. L.: Diode laser cavity ring-down spectroscopy for in situ measurement of NO3 radical in ambient air, J Quant Spectrosc Ra, 166, 23-29, 10.1016/j.jqsrt.2015.07.005, 2015.

Wang, H. C., and Lu, K. D.: Determination and Parameterization of the Heterogeneous Uptake Coefficient of Dinitrogen Pentoxide (N_2O_5), Prog Chem, 28, 917-933, 10.7536/Pc151225, 2016.

Wang, T., Tham, Y. J., Xue, L. K., Li, Q. Y., Zha, Q. Z., Wang, Z., Poon, S. C. N., Dube, W. P., Blake, D. R., Louie, P. K. K., Luk, C. W. Y., Tsui, W., and Brown, S. S.: Observations of nitryl chloride and modeling its source and

effect on ozone in the planetary boundary layer of southern China, J Geophys Res-Atmos, 121, 2476-2489, 10.1002/2015jd024556, 2016.

Wang, H. C., Chen, J., and Lu, K. D.: Development of a portable cavity-enhanced absorption spectrometer for the measurement of ambient NO_3 and N_2O_5: experimental setup, lab characterizations, and field applications in a polluted urban environment, Atmos Meas Tech, 10, 1465-1479, 10.5194/amt-10-1465-2017, 2017a.

Wang, H. C., Lu, K. D., Tan, Z. F., Sun, K., Li, X., Hu, M., Shao, M., Zeng, L. M., Zhu, T., and Zhang, Y. H.: Model simulation of NO_3, N_2O_5 and $ClNO_2$ at a rural site in Beijing during CAREBeijing-2006, Atmos Res, 196, 97-107, 10.1016/j.atmosres.2017.06.013, 2017b.

Wang, H. C., Lu, K. D., Chen, X. R., Zhu, Q. D., Chen, Q., Guo, S., Jiang, M. Q., Li, X., Shang, D. J., Tan, Z. F: High N2O5 concentrations observed in urban Beijing: Implications of a large nitrate formation pathway., Environ. Sci. Technol. Lett., 10, doi: 10.1021/acs.estlett.7b00341, 2017c.

Wang, X. F., Wang, H., Xue, L. K., Wang, T., Wang, L. W., Gu, R. R., Wang, W. H., Tham, Y. J., Wang, Z., Yang, L. X., Chen, J. M., and Wang, W. X.: Observations of N_2O_5 and $ClNO_2$ at a polluted urban surface site in North China: High N_2O_5 uptake coefficients and low $ClNO_2$ product yields, Atmos Environ, 156, 125-134, 10.1016/j.atmosenv.2017.02.035, 2017.

Wang, Z., Wang, W. H., Tham, Y. J., Li, Q. Y., Wang, H., Wen, L., Wang, X. F., and Wang, T.: Fast heterogeneous N_2O_5 uptake and $ClNO_2$ production in power plant and industrial plumes observed in the nocturnal residual layer over the North China Plain, Atmos Chem Phys, 17, 12361-12378, 2017. 10.5194/acp-17-12361-2017

Wayne, R. P., Barnes, I., Biggs, P., Burrows, J. P., Canosamas, C. E., Hjorth, J., Lebras, G., Moortgat, G. K., Perner, D., Poulet, G., Restelli, G., and Sidebottom, H.: The Nitrate Radical - Physics, Chemistry, and the Atmosphere, Atmos Environ a-Gen, 25, 1-203, Doi 10.1016/0960-1686(91)90192-A, 1991.

Xue, L. K., Saunders, S. M., Wang, T., Gao, R., Wang, X. F., Zhang, Q. Z., and Wang, W. X.: Development of a chlorine chemistry module for the Master Chemical Mechanism, Geosci Model Dev, 8, 3151-3162, 10.5194/gmd-8-3151-2015, 2015.

Ye, N. N. L., K. D. Dong, H. B. Wu, Y. S. Zeng, L. M and Zhang, Y. H.: A study of the Water-Soluble Inorgic Salts and Their Gases Precursors at Wangdu Site in the Summer Time, Acta Scientiarum Naturalium Universitatis, 52, p1109-1117, doi.org/10.13209/j.0479-8023.2016.116, 2016.

Yue, D. L., Hu, M., Wu, Z. J., Wang, Z. B., Guo, S., Wehner, B., Nowak, A., Achtert, P., Wiedensohler, A., Jung, J., Kim, Y. J., and Liu, S.: Characteristics of aerosol size distributions and new particle formation in the summer in Beijing, J Geophys Res-Atmos, 114, Artn D00g1210.1029/2008jd010894, 2009.

Zheng, J., Hu, M., Du, Z. F., Shang, D. J., Gong, Z. H., Qin, Y. H., Fang, J. Y., Gu, F. T., Li, M. R., Peng, J. F., Li, J., Zhang, Y. Q., Huang, X. F., He, L. Y., Wu, Y. S., and Guo, S.: Influence of biomass burning from South Asia at a high-altitude mountain receptor site in China, Atmos Chem Phys, 17, 6853-6864, 10.5194/acp-17-6853-2017, 2017.

Figure 1. Map of Beijing and surrounding area. The red star shows the location of the Changping site, and red dots show other sites where previous N_2O_5 measurements were conducted in the North China Plain (NCP), including Wangdu, Jinan and Mt. Tai (Tai' an).

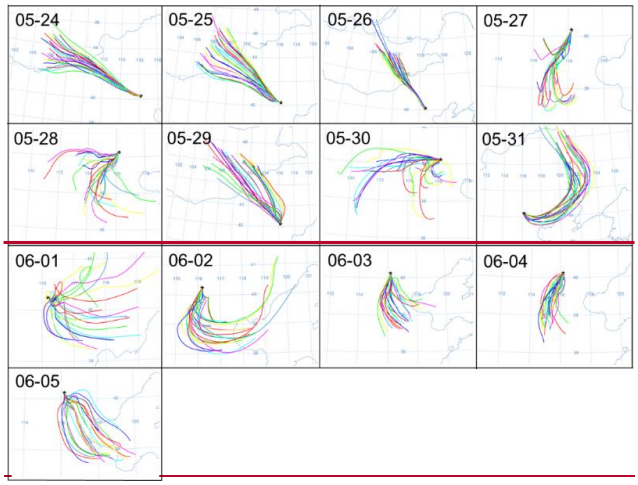

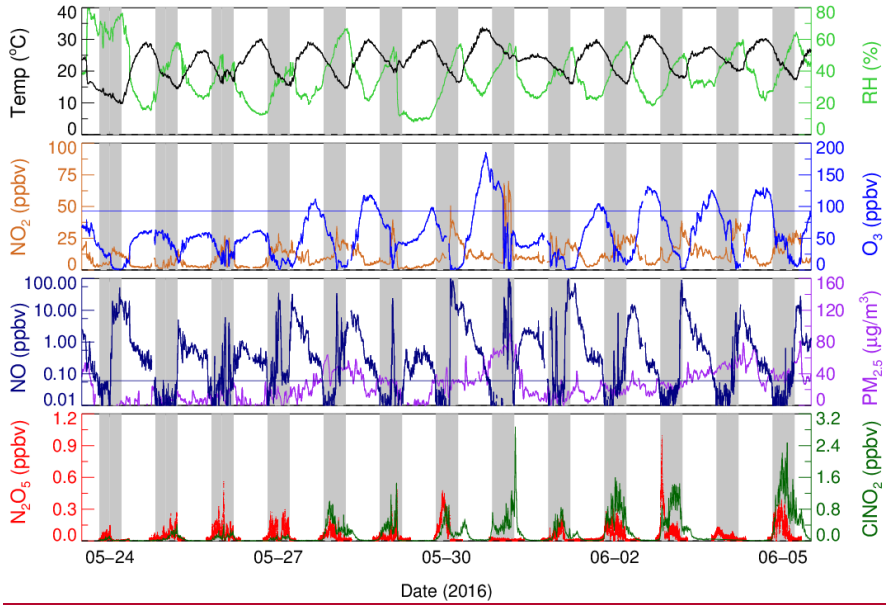

Figure 2. ~~Backward trajectory calculations using the Hybrid Single-Particle Lagrangian Integrated Trajectory (HYSPLIT) model. The images depict a 24-h history of air masses arriving at the measurement site at 12:00 (CNST).~~

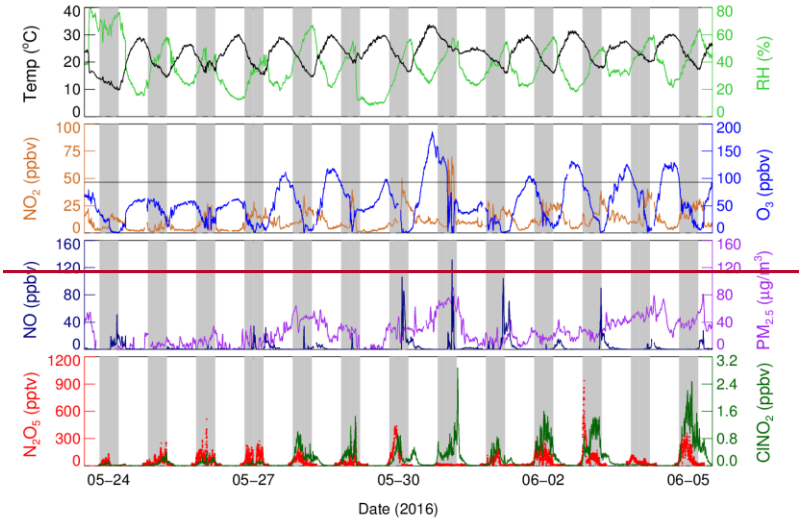

~~**Figure 3.**~~ Time series of N_2O_5, $ClNO_2$ and other relevant parameters. The ~~black~~blue line in the O_3 panel denotes Chinese national air quality standard for O_3 (ca. 93 ppbv for the surface conditions). The black line in the NO panel denotes 0.06 ppbv.

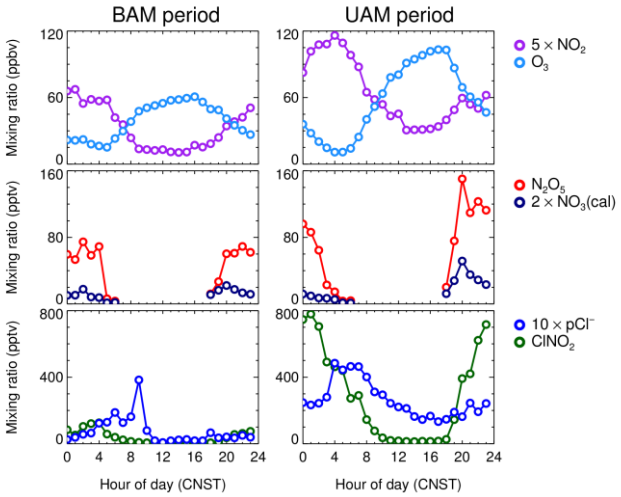

Figure 43. Mean diurnal profiles of $5\times NO_2$, O_3, N_2O_5, $2\times NO_3$ (calculated), $ClNO_2$, and $10\times pCl^-$. The left three panels depict the background air mass (BAM) period and the right three panels depict the urban air mass (UAM) period.

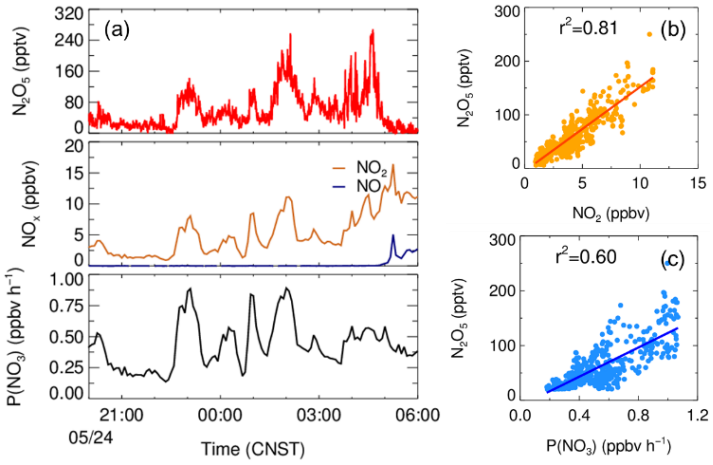

Figure ~~54~~. The correlation of the mixing ratio of N_2O_5 and NO_2 and the production rate of NO_3 on the night of May 24.

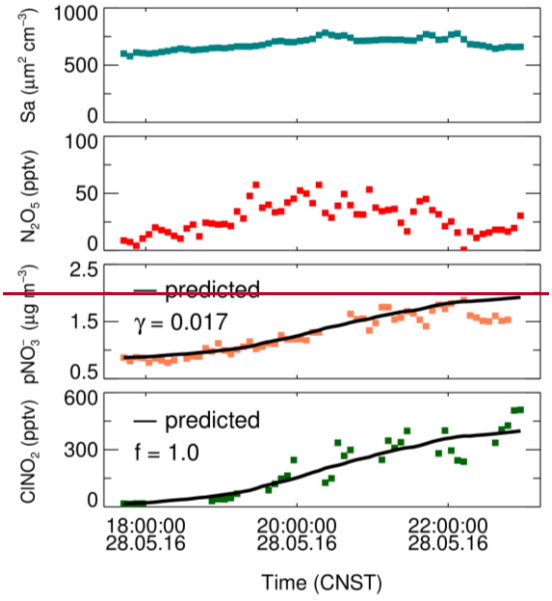

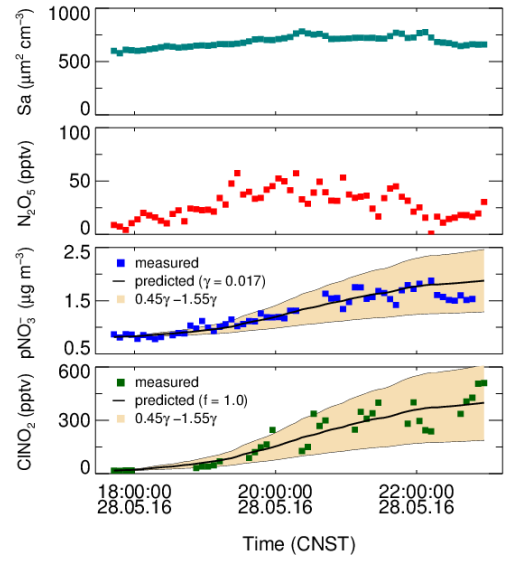

Figure ~~6~~5. The best fit of γ and f to reproduce the observed $ClNO_2$ and pNO_3^- with an offset on May 28. The black lines are the predicted results of the integrated NO_3^- and $ClNO_2$ by using the observed S_a and N_2O_5.

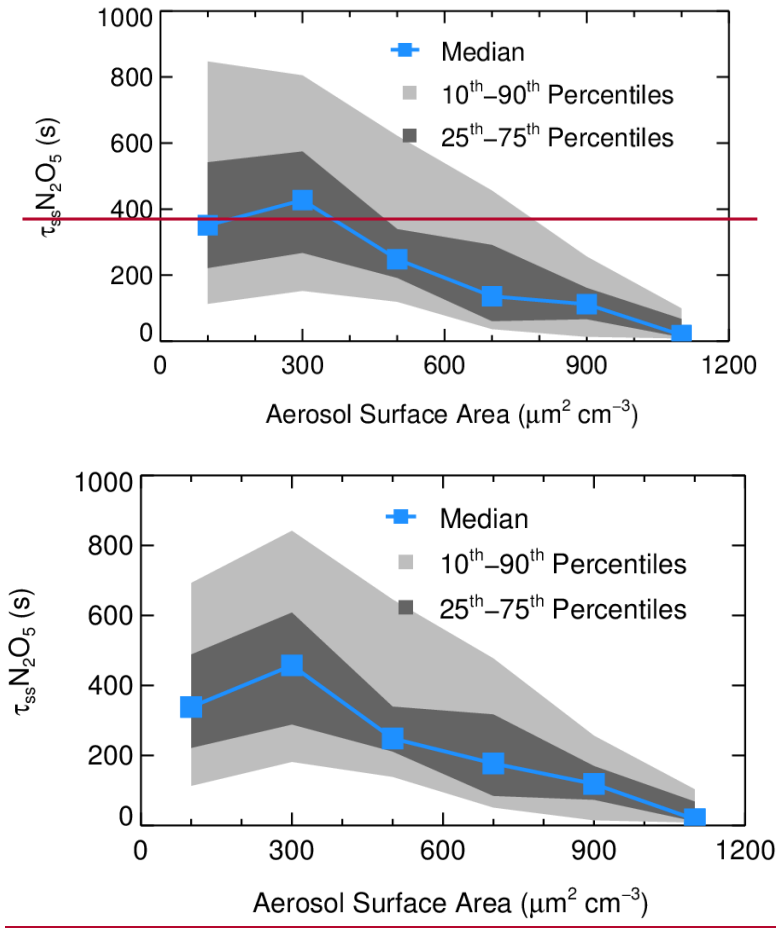

Figure ~~7~~6. The dependence of N_2O_5 lifetime on aerosol surface area. Data were selected from 20:00 to 04:00 and are shown as medians, 25 - 75th percentile ranges, and 10 - 90th percentile ranges, as shown in the legend.

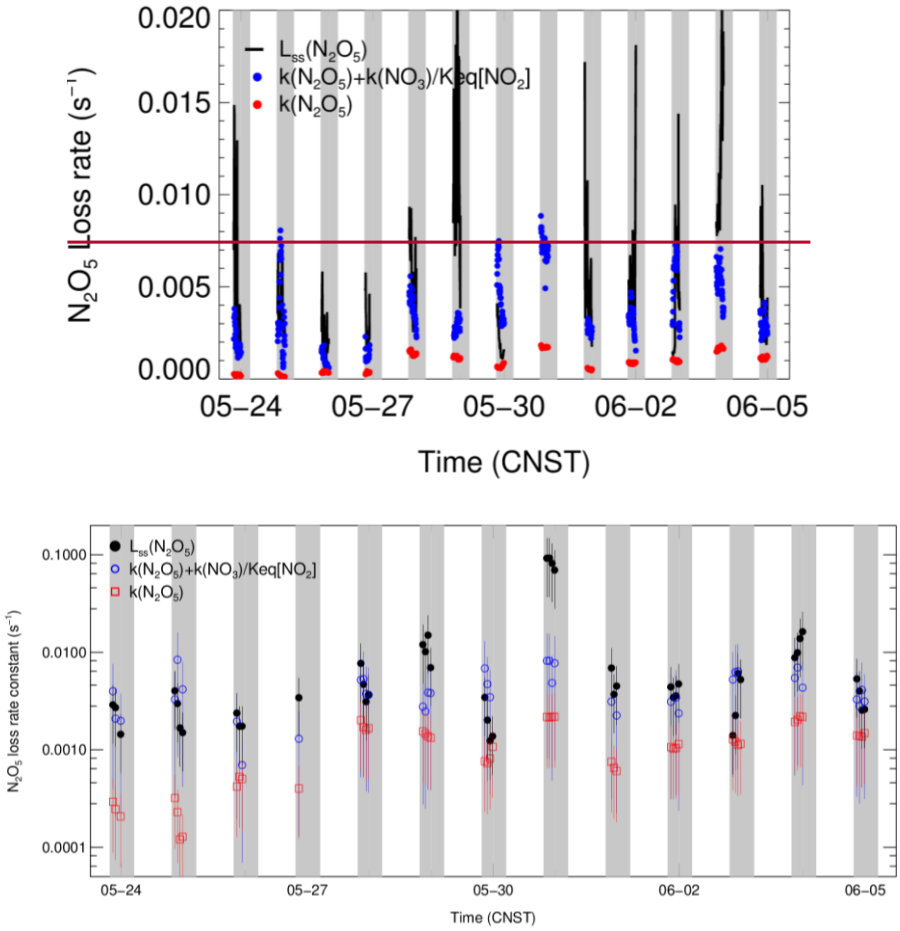

Figure 87. Time series of the individual N_2O_5 loss terms and the loss rate constant of N_2O_5 in steady state (*Lss*(N_2O_5)).

带格式的：字体：三号

带格式的：fontstyle01

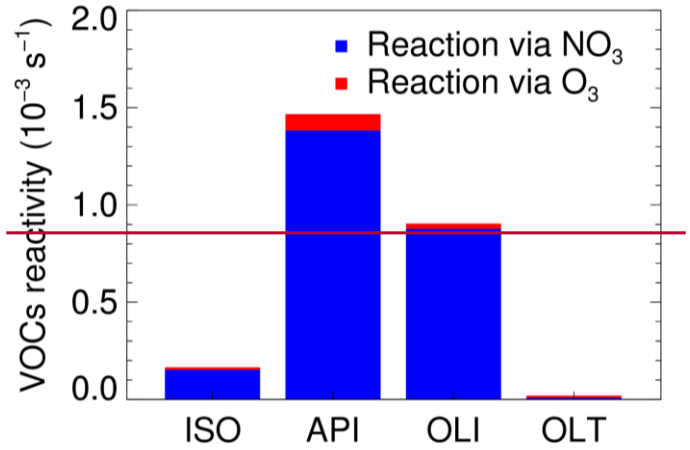

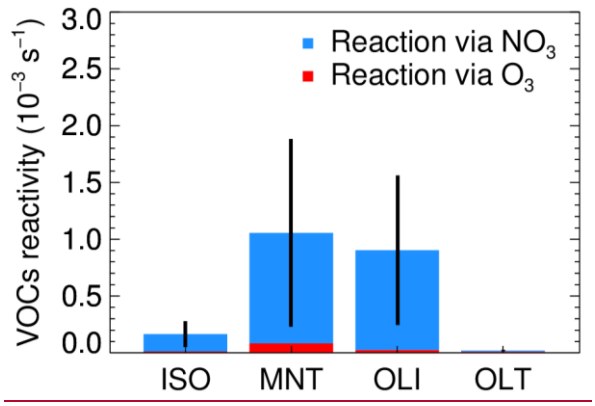

Figure ~~9~~8. The nighttime VOCs reactivity of NO_3 and O_3~~;~~ (defined as the ~~classification was based on RACM2,~~pseudo first order loss rate of VOCs initialed by oxidants, include NO_3 and O_3); the VOCs are classified as isoprene (ISO), monoterpene (MNT), the terminal alkenes (OLT) and the internal alkenes (OLI). The data were selected from 20:00 to the next day 04:00.

带格式的：字体：加粗

带格式的：fontstyle01

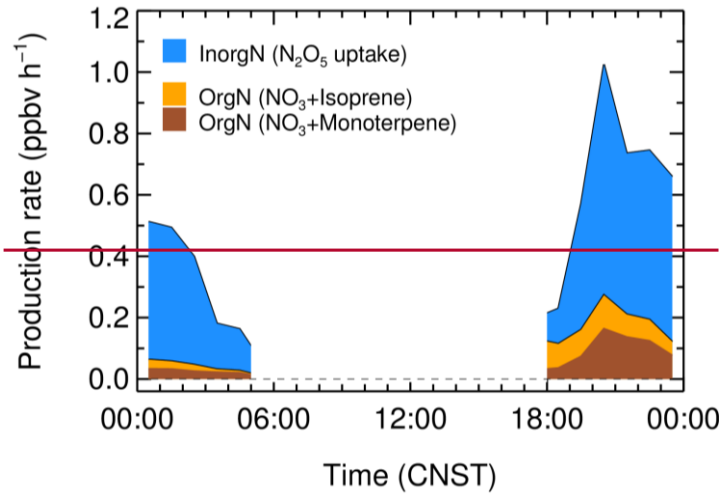

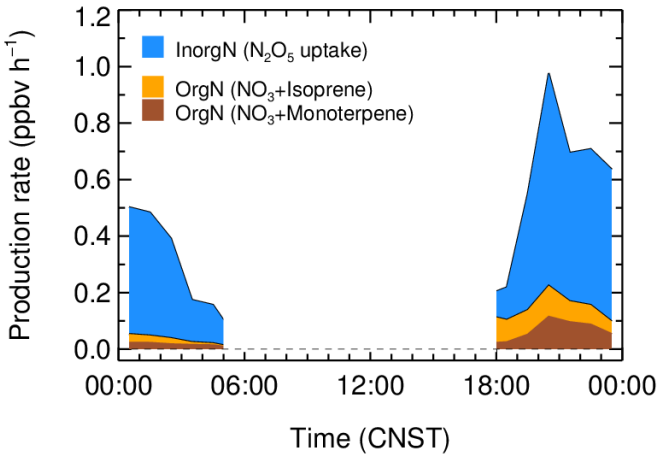

Figure ~~10~~9. The nighttime production rate of organic and inorganic nitrates; the inorganic nitrates were calculated from the N_2O_5 heterogeneous hydrolysis, and the ONs were calculated by the NO_3 reacted with isoprene and monoterpene.

Table 1. The observed gas and particle parameters used in this analysis during the campaign.

Species	Limit of detection	Methods	Accuracy
N_2O_5	2.7 pptv (1σ, 1 min)	CEAS	± 19%
$ClNO_2$	16 pptv (2σ, 1 min)	FIGAERO-ToF-CIMS	± 23%
NO	60 pptv (2σ, 1 min)	Chemiluminescence	± 20%
NO_2	0.3 ppbv (2σ, 1 min)	Mo convert	± ~~20~~50%
O_3	0.5 ppbv (2σ, 1 min)	UV photometry	± 5%
Aerosol surface area	- (4 min)	SMPS, APS	± 30%
VOCs	0.1 ppbv (5 min)	PTR-MS	± 30%
$PM_{2.5}$	0.1 μg m^{-3} (1 min)	TEOM	± 5%
$PM_{1.0}$ components	0.15 μg m^{-3} (4 min)	HR-ToF-AMS	± 30%

Table 2. Summary of the field observed ambient $ClNO_2/N_2O_5$.

Location	Region	$ClNO_2/N_2O_5$ [a]	References
Beijing, China	Inland	0.7 – 42.0 (5.4)	This work
Wangdu, China	Inland	0.4 - 131.3 (29.5)	Tham et al., 2016
Jinan, China	Marine	25.0 - 118.0 [b]	~~Z~~X. F. Wang et al., 2017
Mt. Tai, China	Marine	~ 4.0	~~X.F~~Z. Wang et al., 2017
Hong Kong, China	Marine	0.1 - 2.0	T. Wang et al., 2016
London, UK	Inland	0.02 - 2.4 (0.51)	Bannan et al., 2015
Frankfurt, Germany	Inland	0.2 - 3.0	Phillips et al., 2012
Colorado, USA	Inland	0.2 - 3.0	Thornton et al., 2010
California, USA	Marine	~ 0.2 - 10.0 [c]	Mielke et al., 2013

Note: [a] Daily average results; [b] Power plant plume cases at Mt. Tai in Shandong, China; [c] Estimated according to Mielke et al., (2013).

Table 3. Summary of the average $\gamma \times f$ values derived in the field observations.

Location	Region	$\gamma \times f$	References
Beijing, China	suburban	0.019 ± 0.009	This work
Frankfurt, Germany	suburban	0.014	Phillips et al., 2016
Mt. Tai, China	suburban	0.016	~~X.F~~Z. Wang et al., 2017
Jinan, China	urban	<0.008	~~Z~~X. F. Wang et al., 2017
California, USA	urban	0.008	Mielke et al., 2013

带格式表格

Table 4. List of the N_2O_5 uptake coefficients and the yield of $ClNO_2$ in this campaign.

Start time	End time	γ	f
05/25 00:00	05/25 05:00	0.047 ± 0.023	0.60 ± 0.30
05/25 18:30	05/25 23:00	0.012 ± 0.006	1.0 ± 0.50
05/27 19:00	05/27 20:40	0.040 ± 0.032	0.50 ± 0.40
05/28 19:00	05/28 23:00	0.017 ± 0.009	1.0 ± 0.50
05/30 21:00	05/31 00:00	0.055 ± 0.030	0.55 ± 0.30